ADDIS ABABA UNIVERSITY

ADDISABABA INSTITUTE OF TECHNOLOGY

SCHOOL OF MECHANICAL AND INDUSTRIAL ENGINEERING

GRADUATE PROGRAM IN RAILWAY ENGINEERING

OPTIMUM DESIGN OF LOCOMOTIVE DISK BRAKE BY USING FINITE ELEMENT METHOD

A RESEARCH PAPER SUBMITTED TO THE ADDIS ABABA INSTITUTE OF

TECHNOLOGY, SCHOOL OF GRADUATE STUDIES, ADDIS ABABA UNIVERSITY FOR PARTIAL FULFILLMENT OF THE REQUIREMENTS FOR MASTER OF SCIENCE IN ROLLING STOCK ENGINEERING.

BY

TIRUNEH KINDE TIRFE

ADVISOR

DR.ING:- DEMIS ALEMU

May, 2015

Declaration

I, The Undersigned, Declare That This Thesis Is My Original Work, Has Not Been Presented For A Degree In This Or Other University And That All Sources Of Materials Used For This Have Been Acknowledged.

Tiruneh kinde	_____	_____
Name	Signature	Date

Place Addis Ababa Institute of Technology, Addis Ababa University, Addis Ababa, Ethiopia

May, 2015

ADDIS ABABA UNIVERSITY

ADDISABABA INSTITUTE OF TECHNOLOGY

SCHOOL OF MECHANICAL AND INDUSTRIAL ENGINEERING

GRADUATE PROGRAM IN RAILWAY ENGINEERING

Optimum Design of Locomotive Disk Brake by Using Finite Element Method

By

Tiruneh Kinde Tirfe

May, 2015

Approved By Board of Examiners

1. Dr.Ing:- Demis Alemu	_____	_____
Adviser	Signature	Date
2. Habtamu Tikubet (M.Sc)	_____	_____
Internal Examiner	Signature	Date
3. Tsegaye Feleke (M.Sc)	_____	_____
External Examiner	Signature	Date
4. Dr.Birhanu Besha	_____	_____
Rail Way Center Head	Signature	Date

ACKNOWLEDGEMENTS

I would like to thank my M.Sc. Thesis Advisor Dr.Ing Demis Alemu for his support and guidance. I am using this opportunity to express my gratitude to everyone who supported me throughout the course of this M.Sc. Thesis. I am thankful for their aspiring guidance, invaluably constructive criticism and friendly advice during the Thesis work. I am sincerely grateful to them for sharing their truthful and illuminating views on a number of issues related to the thesis. Finally thanks to you all who provided me with the facilities being required and conductive conditions for my MSc thesis.

ABSTRACT

A transient analysis for the thermo elastic contact problem of the locomotive disk brakes with heat generation is performed using the finite element analysis. To analyze the thermo elastic phenomenon occurring in the locomotive disk brakes, the occupied heat conduction and elastic equations are solved with contact problems. The numerical simulation for the thermo elastic behavior of locomotive disk brake is obtained in the repeated brake condition. The computational results are presented for the distribution of heat flux and temperature on each friction surface between the contacting bodies. Also, thermo elastic instability (TIE) phenomenon (the unstable growth of contact pressure and temperature) is investigated in the present study, and the influence of the material properties on the thermo elastic behaviors (the maximum temperature on the friction surfaces) is investigated to facilitate the conceptual design of the disk brake system. Based on these numerical results, the thermo elastic behaviors of the four brake materials are discussed and stainless steel with excellent mechanical and thermal properties is selected for design purpose.

Table of Contents pages

Acknowledgment i
Abstract ii
Table Of Contents iii
List Of Figures v
List Of Tables vii
Nomenclatures vii
Subscripts viii
Chapter 1: Introduction 1
1.2 Classification Of Brakes 1
1.3 Disc Brake 2
1.3.1 Swinging Caliper Disc Brakes 2
1.3.2 Sliding Caliper Disc Brake 3
1.4 Problems In Locomotive Disc Brake 3
1.5 Objective of the Present Study 3
1.5.1 General Objective 3
1.5.2 Specific Objective 4
1.6 Methodology 4
1.6.1 Data and Data Source 4
1.6.2 Method Of Data Collection 4
1.6.3 Method of Analysis 4
1.6.4 Research method 4
1.7 Organization of the Research 5
1.8 Limitations 5
1.8 Significant And Beneficiaries Of The Research 6
Chapter 2: Literature Review 7
Chapter 3: Modeling Thermo Mechanical Effects In Railway Disc Brake 18
3.1 Operating And Technical Condition Of Locomotive 18
3.2 Theoretical Approaches to Railway Disc Braking Condition 20
3.2.1 Locomotive Braking and Angular Velocity 20
3.2.2 Braking Energy Of Locomotive 22
3.2.3 Heat Energy 24

3.2.4 Work Of Friction Force 24
3.2.5 Heat Flux Entering the Disc 25
3.2.6 Centrifugal Force Of The Disc 26
3.2.7 Determination of Friction Surfaces of the Disc 26
3.2.8 Determination Of Heat Flux And Brake Disc Force 27
3.2.9 Force (Surface Pressure) Determination for the Brake Caliper 27
3.3 Procedure For Fem Analysis With Ansys 28
3.3.1 Build the Model 28
3.3.2 Material Properties 28
3.3.3 Solution Steps on Finite Element Analysis 28
3.4 Finite Element Formulation For Heat Conduction 32
3.5 Thermal Analyses 35
3.6 Structural Analysis 36
Chapter 4: Modeling And Analysis 38
4.1 Definition Of Problem Domain 39
4.2 Creating Finite Element Mesh 39
4.3 Solid Element Geometry 40
4.4 Applying the Boundary Conditions 41
4.4.1 Thermal Boundary Conditions 41
4.4.2 Structural Boundary Conditions 42
4.5 Solution Description In Detail On Modeling And Analysis 42
Chapter 5: Result And Discussion 42
5.1 Candidate Material Properties For The Disc Brake Rotor 43
5.2 Validations of Results 43
5.3 Thermo Elastic Behavior In Contact Between Pad And Disc Brake Application 44
Chapter 6: Conclusions and Recommendations 65
6.1 conclusions 65
6.2 Recommendations 67
Reference 68

List of Figures

Figure No.	Description	Page No.
1.1	Assembly of locomotive Disk brake and pads	**2**
3.1	Electric Locomotives model HX1C	**18**
3.2	Heat input during braking stop	**25**
3.3	boundary conditions of transient heat	**33**
4.1	Model of 30 mm solid Disk brake	**39**
4.2	3-D solid disk Meshed Model	**40**
4.3	Thermal model of solid Disk brake	**41**
4.4	Structural model of solid Disk brake	**42**
5.1	Heat Flux distribution of disc brake radius on friction surfaces during 8^{th}sec braking step	**44**
5.2	Temperature distribution of disc brake radius on friction surfaces during 8^{th}sec braking step	**47**
5.3	Heat Flux distribution of 30 mm high carbon cast iron disk radius on friction surfaces of disk brake in various braking step	**47**
5.4	Heat Flux distribution of stainless steel disk radius on friction surfaces in various braking step	**48**
5.5	Heat Flux distribution of 30 mm carbon/carbon composite disk radius on Friction surfaces in various braking step	**48**
5.6	Heat Flux distribution of 30 mm silicon carbide disk radius on friction surfaces in various braking step	**49**
5.7	Temperature distribution of 30 mm high carbon cast iron disk radius on Friction surfaces in various braking step	**50**
5.8	Temperature distribution of 30 mm stainless steel disk radius on Friction surfaces in various braking step	**51**
5.9	Temperature distribution of 30 mm carbon/carbon composite disk radius on Friction surfaces in various braking step	**52**

Figure No.	Description	Page No.
5.11	Heat Flux distribution of Isentropic 30 mm high carbon cast iron disk radius on Friction surfaces in two braking step	**53**
5.12	Heat Flux distribution of Orthotropic,30 mm high carbon cast iron disc radius on Friction surfaces in two braking step	**54**
5.13	Temperature distribution of isentropic,30mm high carbon cast iron disc radius on friction surfaces in two braking step	**54**
5.14	Temperature distribution of Orthotropic,30 mm high carbon cast iron disk radius on friction surfaces two braking step	**55**
5.15	Transient temperature distribution of the four different materials on friction surfaces in various operating braking time at 300	**55**
5.16	Temperature contours of 30 mm high carbon Cast Iron disk	**56**
5.17	Temperature contours of 30 mm stainless steel disk	**57**
5.18	Temperature contours of 30 mm Carbon/carbon composite disk	**57**
5.19	Temperature contours of 30 mm silicon carbide disk	**58**
5.2	Distribution of Von misses Stress in 30 mm high carbon Cast iron Disk	**58**
5.21	Distribution of Hoop Stress in 30 mm high carbon Cast iron	**59**
5.22	Distribution of Von misses Stress in 30 mm Stainless Steel Disk	**59**
5.23	Distribution of Hoop Stress in 30 mm Stainless Steel Disk	**60**
5.24	Distribution of Von misses Stress in 30 mm Carbon/carbon composite Disk	**60**
5.25	Distribution of Hoop Stress in 30 mm Carbon/carbon composite Disk	**61**
5.26	Distribution of Von misses Stress in 30 mm silicon carbide Disk	**61**
5.27	Distribution of Hoop Stress in 30 mm silicon carbide Disk	**62**
5.28	Average displacement in 30mm high carbon Cast Iron Disk	**62**
5.29	Average displacement in 30 mm Stainless Steel Disk	**63**
5.3	Average displacement in 30mm Carbon/carbon composite Disk	**63**
5.31	Average displacement in 30mm Silicon carbide Disk	**64**

List of tables

Table No.	Description	Page No.
3.1	Main technical parameters	19
3.2	for heat flux calculating Data	22
3.3	Dimension of disc and brake pad for railway locomotives	27
3.4	Shows The Brief Descriptions Steps Followed In Each Phase	29
5.1	Material Property Of High Carbon Cast Iron	45
5.2	Material Property Of Stainless Steel	45
5.3	Material Property Of Carbon/Carbon Composite	46
5.4	Material Property Of Silicon Carbide	46
5.5	Isentropic, High Carbon Cast Iron	51
6.1	Conclusions Of Material Result	66
6.2	Allowable Values Of Standard Materials	66

Nomenclature

c Specific heat (J/kg K)

C Capacity matrix

D Elasticity matrix

E Young's modulus (N/mm^2)

h Heat convection coefficient (W/m^2K)

k Thermal conductivity (W/m K)

K Conductivity matrix

P Normal pressure (N/ mm^2

f Force vector

P_h Hydraulic pressure (N/ mm^2)

q	Heat flux (W/ m^2)
r, > z	Cylindrical coordinates
R	Heat source vector
T	Temperature (K)
T∞	Ambient temperature (K)
U	Displacement vector normal component of displacements
α	Thermal expansion coefficient (/Ċ)
ε	Strain vector
μ	Coefficient of friction
v	Poisson ratio
Þ	Density (Kg /m^3)
σ	Stress vector
ω	Angular velocity (rad/s)

Subscripts

f	Body force
i,j	Sub regions i and j, respectively
n	Normal direction surface traction
ΔT	Temperature rise (K)

CHAPTER 1:

INTRODUCTION

A brake is a device by means of which artificial frictional resistance is applied to moving machine member, in order to stop the motion of a machine. In the process of performing this function, the brakes absorb either kinetic energy of the moving member or the potential energy given up by objects being lowered by hoists, elevators etc. The energy absorbed by brakes is dissipated in the form of heat. This heat is dissipated in the surrounding atmosphere to stop the vehicle, so the brake system should have following requirements.

- The brakes must be strong enough to stop the locomotive within a minimum distance in an emergency.
- The driver must have proper control over the locomotive during braking and locomotive must not skid.
- The brakes must have well anti fade characteristics i.e. their effectiveness should not decrease with constant prolonged application.
- The brakes should have well anti wear properties

1.2. CLASSIFICATION OF BRAKES

The mechanical brakes according to the direction of acting force may be divided into the following two groups:

- Radial brake
- Axial brake

Radial brake

In these brakes the force acting on the brakes drum is in radial direction. The radial brakes may be subdivided into external brakes and internal brakes.

Axial brake

In these brakes the force acting on the brake drum is only in the axial direction. I.e. Disk brakes, cone brakes

1.3. Disc brake

A disk brake consists of a cast iron disk bolted to the wheel hub and a stationary housing called caliper. The caliper is connected to some stationary part of the vehicle like the axle casing or the stub axle as is cast in two parts each part containing a piston. In between each piston and the disk there is a friction pad held in position by retaining pins, spring plates etc. passages are drilled in the caliper for the fluid to enter or leave each housing. The passages are also connected to another one for bleeding. Each cylinder contains rubber-sealing ring between the cylinder and piston. A schematic diagram is shown in the figure 1.1.

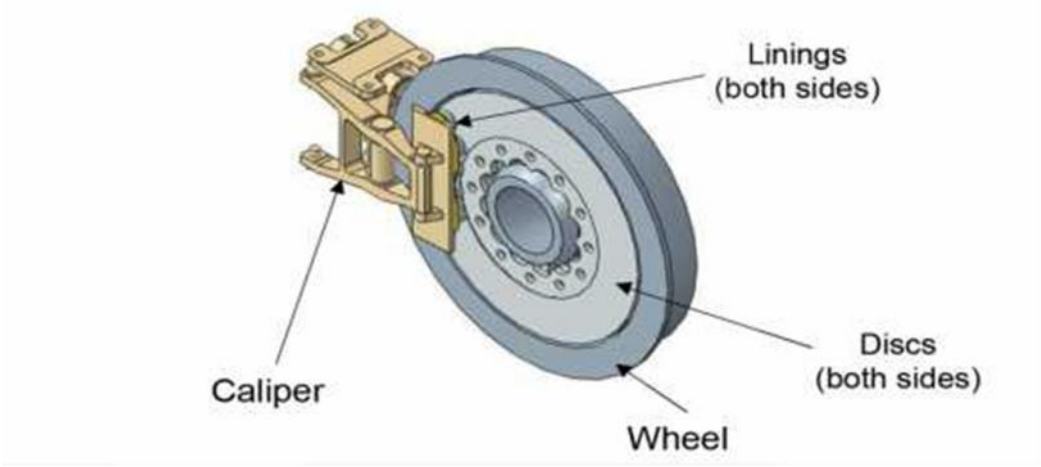

Figure1.1. Assembly of Locomotive Disc Brake and Pads

The main components of disc brake are:

- The brake pads
- The caliper which is mouted to the piston
- The rotor which is munted to the hub

When the brakes are applied, hydraulically actuated pistons move the friction pads in to contact with the rotating disk, applying equal and opposite forces on the disk. Due to the friction in between disk and pad surfaces, the kinetic energy of the rotating wheel is converted into heat, by which locomotive is to stop after a certain distance. On releasing the brakes the rubber-sealing ring acts as return spring and retracts the pistons and the friction pads away from the disk.

1.3.1. Swinging Caliper Disc Brakes

The caliper is hinged about a fulcrum pin and one of the friction pads is fixed to the caliper. The fluid under pressure presses the other pad against the disc to apply the brake. The

reaction on the caliper causes it to move the fixed pad inward slightly applying equal pressure to the other side of the pads. The caliper automatically adjusts its position by swinging about the pin.

1.3.2. Sliding Caliper Disk Brake:

These are two pistons between which the fluid under pressure is sent which press one friction pad directly on to the disc whereas the other pad is passed indirectly via the caliper.

1.4. Problems in Locomotive Disk Brake

In the course of brake operation, frictional heat is dissipated mostly into pads and a disk, and an occasional uneven temperature distribution on the components could induce severe thermo elastic distortion of the disk. The thermal distortion of a normally flat surface into a highly deformed state, called thermo elastic transition. It sometimes occurs in a sequence of stable continuously related states operating conditions change. At other times, however, the stable evolution behavior of the sliding system crosses a threshold whereupon a sudden change of contact conditions occurs as the result of instability. This invokes a feedback loop that comprises the localized elevation of frictional heating, the resultant localized bulging, a localized pressure increases as the result of bulging, and further elevation of frictional heating as the result of the pressure increase. When this process leads to an accelerated change of contact pressure distribution, the unexpected hot roughness of thermal distortion may grow unstably under some conditions, resulting in local hot spots and leaving thermal cracks on the disk. This is known as thermo elastic instability (TEI). The thermo elastic instability phenomenon occurs more easily as the rotating Speed of the disk increases. This region where the contact load is concentrated reaches very high temperatures, which cause deterioration in braking performance. Moreover, in the course of their presence on the disk, the passage of thermally distorted hot spots moving under the brake pads causes low-frequency brake vibration

1.5. Objective of the Present Study

1.5.1. General objective

The main objective of the thesis to recommend optimal material for train disk brake that give

minimum stress and temperature in the disk.

1.5.2. Specific Objective

The specific objectives are:

- To identify materials for disc, their stresses and thermal properties
- To model mechanical loads on disc
- To analyze the temperature and stress distribution on disc for each of identified materials
- To recommend the optimal materials by analyzing the result

1.6 Methodology

1.6.1 Data and Data source

Primary and secondary data from ERC and other sources will also be used.

1.6.2 Method of data collection

The data will be collected using different tools like

- Tables
- Figures/Graphs
- Charts and others

1.6.3 Method of Analysis

Quantitative data analysis technique and will make analysis using Simulation software called Ansys will be used.

1.6.4 Research Method

A lot of journal and paper has been read up and part of it has been considered in this project. Meanwhile, the actual real brake disc dimension has been taken from ERC specification for analysis purpose. Later, the precise dimensions have been drawn in ansys APDL software for further analysis.

Next, the 3D model of disc brake rotor has been drawn by finite element software which is ANSYS software. Thermal analysis will be done on transient responses. Assigning material

properties, load and meshing of the model will be done in ANSYS software. Finally an expected result of thermal analysis will be obtained.

Finally, the performance and safety factor of optimum design of the disc brake will be analyzed based on the Ansys analysis result of thermal nodal temperature and structurally all the stresses will be calculated on the demand of the candidate materials accordingly.

So that from the result, this research checks the performance and safety factor optimum design of disc brake systems and from that the research decide what materials are best for train braking comparing from the candidate materials during braking application.

1.7 Organization of the Research

The research is organized in seven parts. The first chapter is the introduction part which clearly states the introduction of the disc brake, statement of problem, and objective, scope and limitation of the study, methodology, and benefits of the research.

Chapter two discusses Literature review of the disc brake system of rail vehicle. Which are written and discussed by various researchers such as definition, key points, and analytical approaches will be discussed in this part of the study.

Chapter three shows the data collection and interpretation with data collection results, physical model and procedures of ansys work.

The solid model of disc brake and analysis of train disc brake as well as the material and boundary conditions are discussed in detail under chapter four.

Chapter five deals about Ansys result and discussion of the result obtained after the simulation process using Ansys. This is done using numerical approach.

Conclusion and Recommendation are discussed in chapter six showing of the results in table and also allowable stresses of the materials.of the research on railroad vehicle brake system will be discussed and forwarded. This will be the final chapter of the research.

1.8. Limitation

To graph and visualize the transient property of the four different materials' result into one x-y axis using time history post processor of ansys software is difficult, so I am working by doing the individual result from time history post processor of ansys software then copying into excel

until the four materials are completed and finally combing these result to get the four graphs effect into excel this somehow makes me difficult to work.

And also working model from other software and then importing into APDL ansys is difficult to get full complete model. These are the basic limitations in my MSc thesis.

1.9. Significant and Beneficiaries of the Research

As a research, the primary merits of the study goes to Ethiopian Railway Corporation. The present study can also provide a useful design tool and improve the brake performance and efficiencies of disk brake system. The paper also will be used for future research center. Since there are a lot of studies have to be done in the area, it will give a comprehensive starting point for more advanced researches. This will also develop awareness for the importance of research center in this field.

CHAPTER 2:

LITRATURE REVIEW

In order to study the transient thermo elastic behavior of the disk brake, the literature related to the thermo-elastic analysis of clutch, two sliding surfaces and brakes have been studied. Since in the past most of the studies of brake and clutch is carried out for thermo elastic analysis by considering it as a case of two dimensional. The following section details the literature available and relevant to the proposed study of transient thermo elastic analysis of a solid disk brake, as a case of three dimensional.

Brilla et al [1] generalized variational principles in the sense of the Laplace transform for viscoelastic problems were derived. Then mathematical theory of viscoelasticity in generalized Hardy spaces and in weighted anisotropic Sobolevspaces and spectral theory of corresponding non-self adjoint operators was elaborated. Finally the Laplace transform FEM for numerical analysis of time-dependent problems of the mathematical physics was proposed and analyzed.

Lin et al [2] determined Radial transient heat conduction in composite hollow cylinders with the temperature-dependent thermal conductivity was investigated numerically by using an application of the Laplace transform technique combined with the finite element method(FEM) or with the finite difference method (FDM). The domain of the governing equation was discretized using the FEM or FDM. The nonlinear terms were linear zed by Taylor's series approximation. The time-derivatives in the linear zed equations were transformed to the corresponding algebraic terms by the application of the Laplace transform. The numerical inversion of the Laplace transform was applied to invert the transformed temperatures to the temperatures in the physical quantity. Since the present method was not a time-stepping procedure, the results at a specific time can be calculated in the time domain without any step-by- step computations. To show the accuracy of the present method for the problems under consideration, a comparison of the hybrid finite element solutions with the hybrid finite difference solutions was made.

Kennedy et al [3] determined the numerical and experimental methods applied to tribology. He

improved the techniques for Finite Element Analysis of sliding surface temperature. Essential component of manually operated vehicle transmissions is the synchronizer. Synchronizers have the task of minimizing the speed difference between the shifted gearwheel and the shaft by means of frictional torque before engaging the gear. Proper operation requires a sufficiently high coefficient of friction. It is common practice to investigate the friction and wear behavior under various loading conditions on test rigs or in vehicle tests. An optimized design of the system with regard to appropriate function and durability on the one hand as well as low cost, low mass and compact over- all dimensions on the other hand requires extensive testing. According to the present state of knowledge, derived from numerous experimental investigations, temperature can be attributed the most significant influence on the tribology of synchronizing systems. Therefore, the influence of various loading conditions on contact temperature was investigated; a relation between temperature and tribological performance was established. The Finite Element Method was applied to simulate the thermal behavior of a synchronizing system depending on different operating conditions. A result of this simulation is the spatial and time-dependent temperature distribution in the area of contact. Characteristics of the tribological performance of a molybdenum coated synchromesh ring in contact with a steel cone were derived from extensive experimental investigations. Significantly different friction and wear patterns can be distinguished. At heavy loading conditions the coefficient of friction is quite high and continuously severe wear occurs; light operating conditions results in a low friction coefficient, whilst no more wear is observed. Between those two extremes an indifferent regime exists, in which both patterns of tribological behavior occur A reason for this characteristics behavior of the system described here was found by means of the Finite Element simulation. Apparently, the friction and wear pattern depends on the temperature in the contact area; for mild wear and low friction coefficients the contact temperature must not exceed a critical value in order to avoid severe wear. Within limits the predicted tribological behavior and the test results are in good agreement. The calculation of the temperature in the contact area provides a basis for a classification of the load conditions in terms of their thermal and tribological effect, a practically applicable estimation of service life and a design procedure based on numerical simulation rather than on testing.

Tsinopoulos et al [4] determined an advanced boundary element method was appropriately

combined with the fast Fourier transform (FFT) to analyze general axisymmetric problems in frequency domain electrodynamics. The problems were characterized by axisymmetric geometry and non-axisymmetric boundary conditions. Boundary quantities were expanded in complex Fourier series in the circumferential direction and the problem was efficiently decomposed into a series of problems, which were solved by the BEM for the Fourier boundary quantities, discrediting only the surface generator of the axisymmetric body. Quadratic boundary elements were used and BEM integrations were done by FFT algorithm in the circumferential direction and by Gauss quadrature in the generator direction. Singular integrals were evaluated directly in a highly accurate way. The Fourier transformed solution was then numerically inverted by the FFT provided the final solution. The method combines high accuracy and efficiency and this was demonstrated by illustrative numerical examples.

Gonaska et al [5] determined the four automotive friction system hot spot types were introduced and discussed. These were asperity, focal, distortional, and regional. Friction material and metal counter surface wear consequences were discussed, as they related to the different hot spotting types. Focal hot spots were emphasized. These may form martensite on the cast iron drum or disk rubbing surface. Such hot spots, if not prevented, can provide a root cause for unacceptable performance or durability in automotive friction systems. Computer studies, using a two-dimensional model, were used to complement the experimental studies of critical hot spots and determine hot spot thermal flux limits. Surface melting and known requirements for the formation of martensite were used to establish bounds from the computer analysis.

Floquet et al [6] determined of temperature distribution and comparison of simulation results and experimental results in the disc by 2D thermal analysis using axisymmetric model. The disc brake used in the automobile is divided into two parts; a rotating axisymmetrical disc, and the stationary pads. The friction heat, which is generated on the interface of the disc and pads, can cause high temperature during the braking process. The influence of initial velocity and deceleration on cooling of the brake disc was also investigated. The thermal simulation is used to characterize the temperature field of the disc with appropriate boundary conditions.A Finite-element method was developed for determining the critical sliding speed for thermo elastic instability of an axisymmetric clutch or brake. Linear perturbations on the constant-speed

solution w e r e sought that vary sinusoid ally in the circumferential direction and grow exponentially in time. These factors cancel in the governing thermo elastic and heat-conduction equations, leading to a linear eigenvalue problem on the two- dimensional cross-sectional domain for the exponential growth rate for each Fourier wave number. The imaginary part of this growth rate corresponds to a migration of the perturbation in the circumferential direction. The algorithm was tested against an analytical solution for a layer sliding between two half-planes and provided excellent agreement, for both the critical speed and the ,migration speed. Criteria were developed to determine the mesh re-finement required to give an adequate discreet description of the thermal boundary layer adjacent to the sliding interface. The method was then used to determine the unstable mode and critical speed in geometries approximating current multi-disc clutch practice.

Burton et al [7] showed the thermal deformation in frictionally heated contact wheel-mounted on disc brakes were exposed to severe non-symmetrical mechanical and thermal loads. The paper described the design process for two high-performance, hub-mounted discs of different size and duty. The development was resulted in two very successful but fundamentally different hub designs and manufacturing methods. Initially, finite element analyses used in the design optimization were mainly concentrated on bulk thermal effects Recently, in order further to improve the design process, analyses had included macro thermal effects, providing valuable results particularly related to the prediction of disc permanent coning, one of the most critical design requirements.

Whenever friction occurs in dry sliding of mechanical components, mechanical energy is transformed into heat through surface and volumetric processes in and around the real area of contact. This frictional heating, and the thermal and thermo mechanical phenomena associated with it, can have a very important influence on the tribological behavior of the sliding components, especially at high sliding velocities. Significant developments in the study of these phenomena were reviewed. Among the topics reviewed were mechanisms of frictional heating and the distribution of heat during sliding friction, the measurement and analysis of surface and near surface temperatures resulting from frictional heating, thermal deformation around sliding contacts and the changes in contact geometry caused by thermal deformation and thermo elastic instability, and the thermo mechanical stress

distribution around the frictionally heated and thermally deformed contact spots. The paper concludes with a discussion of the influence of the thermal and thermo mechanical contact Phenomena on wear, thermo cracking and other modes of failure of sliding mechanical components.

Ender son et al [8] investigated the hot spotting in automotive friction system. When sliding occurs with significant frictional heating thermo elastic deformation may lead to a transition from smoothly distributed asperity contact to a condition where the surfaces are supported by a few thermal asperities. This circumstance may be associated with a transition to a condition of severe wear because of the elevated contact pressure and temperature, and also because of production of tensile stresses. This second stress component may lead to heat checking whereupon the rough checked surface acts to abrade the mating material.

Comninou et al [9] determined the stability boundary for the thermo elastic contact of a rectangular elastic block sliding against a rigid wall in the presence of a pressure- dependent thermal contact resistance. This geometry can be seen as intermediate between the idealized 'aldo' rod model continuum solutions for the elastic half-plane. The solution was obtained by comparing the expression for the perturbed boundary condition including frictional heating with that for purely static loading, already solved by Yeo and Barber (1995). The critical sliding speed was obtained as a function of the temperature difference imposed between the wall and the free end. In most cases, frictional heating tends to destabilize the system. However, for certain forms of the resistance-pressure law, the opposite conclusion was reached and the system can be stable for all sliding speeds. The factors influencing transition were discussed, including wear, cooling and hydrodynamic lubrication. The transition state was also discussed with regard to the stress distribution, rate of movement of the contact patches and temperatures.

Barber et al [10,11] developed a procedure based on the Radon transform and elements of distribution theory, to obtain fundamental thermo elastic three-dimensional (3D) solutions for thermal and/or mechanical point sources moving steadily over the surface of a half space. A concentrated heat flux was taken as the thermal source, whereas the mechanical source consists of normal and tangential concentrated loads. It is assumed that the sources move with a constant velocity along a fixed direction. The solutions obtained were exact within the

bounds of Boot coupled thermo-elastic dynamic theory, and results for surface displacements are obtained over the entire speed range (i.e. for sub-Raleigh, super-Raleigh/subsonic, transonic and supersonic source speeds). This problem has relevance to situations in Contact Mechanics, Tribology and Dynamic Fracture, and is especially related to the well-known heat checking problem (thermo-mechanical cracking in an unflawed half-space material from high-speed asperity excitations). Our solution technique fully exploits as auxiliary solutions the ones for the corresponding plane-strain and anti-plane shear problems by reducing the original 3D problem to two separate 2D problems. These problems were uncoupled from each other, with the first problem being thermo elastic and the second one pure elastic. In particular, the auxiliary plane-strain problem was completely analogous to the original problem, not only with regard to the field equations but also with regard to the boundary conditions. This makes the technique employed here more advantageous than other techniques, which require the prior determination of a fictitious auxiliary plane-strain problem through solving an integral equation.

Dow et al [12**]** proposed to contribute to dynamic and thermal analysis of the braking phenomenon. A dynamic model was established. Using this model the equation of motion of a car was derived for straight line braking. In this context, firstly the pressure variations in the brake hydraulic circuit versus pedal force were determined. Afterwards, the expression for friction torques and associated braking force induced by hydraulic pressure was taken into account, and substituted into the equation of motion of vehicle. In its last form, this equation was numerically solved by means of the Newark integration scheme; so, the distance traveled by car until stopping, along with its speed and deceleration, was computed. Finally, a thermal analysis in the brake discs and drum was carried out. An excellent agreement between numerical and test results was observed. In addition, optimal pressure values for which the rear tire do not go to lockup was obtained.

Lee et al [13, 14] determined thermo elastic instability in an automotive disc brake system was investigated experimentally under drag braking conditions. The onset of instability was clearly identifiable through the observation of non-uniformities in temperature measured using embedded thermocouples. A stability boundary was established in temperature/speed space, the critical temperature being attributable to temperature- dependence of the brake

pad material properties. It was also found that the form of the resulting unstable perturbations or Eigen functions changes depending upon the sliding speed and temperature. A finite-element method was developed for determining the critical sliding speed for thermo elastic instability of an axis symmetric clutch or brake. Linear perturbations on the constant-speed solution were sought that vary sinusoid ally in the circumferential direction and grow exponentially in time. These factors cancel in the governing thermo elastic and heat-conduction equations, leading to a linear Eigen value problem on the two-dimensional cross-sectional domain for the exponential growth rate for each Fourier wave number. The imaginary part of this growth rate corresponds to a migration of the perturbation in the circumferential direction. The algorithm was tested against an analytical solution for a layer sliding between two half-plane and gave excellent agreement, for both the critical speed and the migration speed. Criteria were developed to determine the mesh refinement required to give an adequate discrete description of the thermal boundary layer adjacent to the sliding interface. The method was then used to determine the unstable mode and critical speed in geometries approximating current multi-disc clutch practice.

Barber et al [15] determined the frictional heat generated during braking causes thermo elastic distortion that modifies the contact pressure distribution If the sliding speed is. sufficiently high, this can lead to frictionally-excited thermo elastic instability (TEI), characterized by major non-uniformities in pressure and temperature. In automotive applications, a particular area of concern is the relation between thermo elastically induced hot spots in the brake disks and noise and vibration in the brake system. Numerical implementation of Burrton's perturbation analysis for thermo elastic instability in a two-dimensional model provided an extremely efficient method for determining the critical speed in simple sliding systems. In this paper, the two- dimensional model has been extended to an annular three-dimensional disk model in order to consider more realistic brake and clutch geometries and to provide more accurate critical speed. The results showed that the Eigen modes exhibit focal hot spots along the circumference on each side of the disk and the thin disk is more stable than the thick disk when both disk thicknesses are below the optimal thickness.

Du et al [16] determined that the finite element method was used to reduce the problem of thermo elastic instability (TEI) for a brake disk to an Eigen value problem for the critical

speed. Conditioning of the Eigen value problem was improved by performing a preliminary Fourier decomposition of the resulting matrices. Results were also obtained for two- dimensional layer and three-dimensional strip geometries, to explore the effects of Increasing geometric complexity on the critical speeds and the associated mode shapes. The hot spots were generally focal in shape for the three-dimensional models, though modes with several reversals through the width start to become dominant at small axial wave numbers n, including a thermal banding mode corresponding to n = 0. The dominant wavelength (hot spot spacing) and critical speed were not greatly affected by the three- dimensional effects, being well predicted by the two-dimensional analysis except for banding modes. Also, the most significant deviation from the two-dimensional analysis can be approximated as a monotonic interpolation between the two-dimensional critical speeds for plane stress and plane strain as the width of the sliding surface was increased. This suggested that adequate algorithms for design against TEI could be developed based on the simpler two-dimensional analysis.

Leroy et al [17] determined hard coatings were more and more used to improve the mechanical and tribological behavior of surfaces. Thermo mechanical cracking can occur in these coatings when they slide under heavy loads. A two-dimensional model of a finite thickness layered medium submitted to a moving heat source was presented. The analytical solution of the temperature and thermo elastic stress fields was obtained using Fourier transforms. The behavior of each layer was described by transfer-matrices and a relation between the displacement- and stress-vectors is given. The originality of the study was the use of a fast Fourier transform algorithm. With this method, calculation time is reduced, no singularity problems were met in the inverse transform and each parameter (especially the thickness of the layers) can be studied over a wide range.

A transient analysis for thermo elastic contact problem of disk brakes with frictional heat generation was performed using the finite element method. To analyze the thermo elastic phenomenon occurring in disk brakes, the coupled heat conduction and elastic equations were solved with contact problems The numerical simulation for the thermo elastic behavior of disk brake was obtained in the repeated brake condition. The computational results were presented for the distributions of pressure and temperature on each friction surface between the

contacting bodies. Also, thermo elastic instability (TEI) phenomenon (the unstable growth of contact pressure and temperature) was investigated in this study, and the influence of the material properties on the thermo elastic behaviors (the maximum temperature and contact ratio. On the friction surfaces) was investigated to facilitate the conceptual design of the disk brake system. Based on these numerical results, the thermo elastic behaviors of the carbon! Carbon composites with excellent mechanical and thermal properties were also discussed.

Wang et al [18] proposed a new numerical method for the boundary element analysis of axisymmetric bodies. The method was based on complex Fourier series expansion of boundary quantities in circumferential direction, which reduces the boundary element equation to an integral equation in (r-z) plane involving the Fourier coefficients of boundary quantities, where r and z are the co-ordinates of the (r, θ, z) cylindrical co-ordinate system. The kernels appearing in these integral equations can be computed effectively by discrete Fourier transform formulas together with the fast Fourier transform (FFT) algorithm, and the integral equations in (r-z) plane can be solved by Gaussian quadrature, which establishes the Fourier coefficients associated with boundary quantities. The Fourier transform solution can then be inverted into (r, θ, and z) space by using again discrete Fourier transform formulas together with FFT algorithm. In the study, first we presented the formulation of the proposed method which was outlined above. Then, the method was assessed by using three sample problems. A good agreement was observed in the comparisons of the predictions of the method with those available in the literature. It was further found that the proposed method provided considerable saving in computer time compared to existing methods.

Akin et al [19] studied the geometry of two flat plates contacting on a straight common edge with sliding parallel to the line of contact, pressure perturbations on the interface will grow, diminish or remain unchanged. The effects of materials properties, friction coefficient, and sliding speed were delineated. Conditions which lead to a growing disturbance may be thought of as undesirable in that they lead to locally increased contact loading as well as locally increased temperatures Adjacent to the regions of increased pressure are regions of reduced pressure where the surfaces may part, and give rise to leakage when the line of contact is considered to represent the lip of a seal. It was shown that materials sliding on their own kind tend to be stable relative to this phenomenon, while good thermal conductors sliding on

good thermal insulators must always have some characteristic sliding speed above which instability will occur. The objective of this research is to advance a technique for simulating a three dimensional disk brake system, clutches, and mechanical seals.Due to its tremendous time and cost requirements, there are no known works on instability simulation evolving via a stable region, but excellent efforts on determining instability conditions using eigenvalue formulation have been reported by Barber and coworkers [10, 11]. For the purpose of design and analysis, understanding of the both transient behaviors and post- instability is of paramount importance in the industry. Thus, in this study we introduce a potential computation technique.

In this study we discretize the domain using finite elements, enables us to reach a very efficient computation technique that has the ability to invoke a fast transient thermo elastic solution and thermo elastic instability as well. This study proposed the aforementioned technique to shed some light on a possibly fast and practically applicable numerical analysis in the field of frictionally induced thermo mechanical coupled problems, such as a disk brake system, clutches, and mechanical seals. By applying the proposed technique, we solved some temperature and displacement fields for a three -dimensional brake system. However, we did not discuss in a quantitative sense the computation results through comparison with experiments for validation since we have not found appropriate technique to solid-type disk instead of ventilated-type disks, for which experimental data can be found in [13,14]. Authors currently are investigating the application of this technique to a ventilated-type disk problem.

Oder, Reibenschuh, , Lerher, Šraml, Šamec, Potrč, [26] showed a thermal and stress analysis of a brake disc for railway vehicles using the finite element method (FEM). Performed analysis deals with two cases of braking; the first case considers braking to a standstill; the second case considers braking on a hill and maintaining a constant speed. In both cases the main boundary condition is the heat flux on the braking surfaces and the holding force of the brake calipers. In addition the centrifugal load is considered.

Thilak, R.Krishnaraj, Sakthivel, Kanthavel, Deepan Marudachalam , .Palani [28] are determined Transient Thermal and Structural Analysis of the Rotor Disc of Disk Brake is aimed at evaluating the performance of disc brake rotor of a car under severe braking conditions and there by assist in disc rotor design and analysis. An investigation into usage of new materials is

required which improve braking efficiency and provide greater stability to vehicle. This investigation can be done using ANSYS software. ANSYS 11.0 is a dedicated finite element package used for determining the temperature distribution, variation of the Stress and Deformation across the disc brake profile. In the present work, an attempt has been made to investigate the suitable hybrid composite material which is lighter than cast iron and has good Young's modulus, Yield strength and density properties. Aluminum base metal matrix composite and high strength Glass Fiber composites have a promising friction and wear behavior as a Disk brake rotor. The transient thermo elastic analysis of Disc brakes in repeated brake applications has been performed and the results were compared. The suitable material for the braking operation is S2 glass fiber and all the values obtained from the analysis are less than their allowable values. Hence the brake disc design is safe based on the strength and rigidity criteria. By identifying the true design features, the extended service life and long term stability is assured.

CHAPTER 3:

MODELING THERMO-MECHANICAL EFFECTS IN RAILWAY DISC BRAKE

In various research articles different modeling approaches for thermal analysis of disc brakes can be found. The models ranging from one–dimensional, two–dimensional, to complex three dimensional are used. The three–dimensional, axis-symmetrical model of transient heat transfer has been chosen in this paper. It should be noticed that the geometry of a disc brake rotor is axis-symmetrical. In this case the assumption of axis-symmetric heat flux on the friction surface means only time averaged boundary conditions over a rotor revolution.

3.1. Operating and Technical Condition of Locomotive

Technical and operative conditions of locomotive

Figure 3.1 Electric Locomotive Model HXIC

Table 3.1 Main Technical Parameters

Description	**Conditions / Values**
Purpose	Freight Transport
Electric Transmission Method	AC-DC-AC
Gauge	1435mm
Bogie Type	SF6N
Axle Arrangement	CO'-CO'
Wheel Diameter New	1250mm
Wheel Diameter New Half Worn	1200mm
Wheel Diameter New Worn	1150mm
Locomotive Service Weight With Additional Weight	140t
Locomotive Service Weight Without Additional Weight	155t
Axle Load	23t + 2t
Starting Tractive Effort	520KN(23t)
Starting Tractive Effort	570KN(25t)
Continuous Rated Speed Of Locomotive	65Km/hr.(25t)
Continuous Rated Speed Of Locomotive	72km/hr.(23t)
Continuous Tractive Effort Of Locomotive 25t	400KN
Continuous Tractive Effort Of Locomotive Axle Load 23t	370KN
Minimum Radius Of Curvature Negotiable Under The Speed Of 5km/Hr.	125m
Wheel Base	2250mm+2000mm
Locomotive Total Wheel Base	16260mm
Locomotive Length(Distance Between Front And Rear Coupler Centers	22670mm
Maximum Width Of Locomotive Body	3100mm

Table 3.1 Main Technical Parameters

Descriptions	**Conditions / Values**
Maximum Height (Upon Pantographs Dropping)	4760mm
Power System	Ac 25Kv, 50Hz
Brake Model	CCBII brake
Mechanical Brake	wheel disk brake
Maximum Continuous Power At The Wheel Rim Tractive /Regenerative Braking	7200KW
Maximum Electric Braking Force	400KN(25t)
Ambient Temperature	-25Ċ∞ +40Ċ
Preheating Measures Must Be Taken When The Temperature	-25Ċ∞ +40Ċ
Transmission Ratio	6.235(106/17)
Permissible Line Velocity	72Km/hr.
Constant Deceleration During Of Stop Braking	1.2m/s2
Maximum Gradient Of Line	11%

3.2. Theoretical Approach to Railway Disc Braking Condition

In the process of braking of railway vehicles, it is necessary to define a model of a thermal analysis that describes the heating transfer of the heat generated by friction at surfaces which are in contact, between a railway disc and braking pads, through the disc and pads, as well as heat outflow of the whole braking system due to cooling of the surrounding air. For thus purposes, an analytical model for analyzing thermal and mechanical stress effects in braking systems of railway vehicles is utilized and its adopted procedure is presented in this paper [26].

3.2.1. Locomotive Braking and Angular Velocity

Brake Application is defined as an application of the brake that results in a brake force being applied to the vehicle. Brake force is the force applied to the brake disc / pad / braking surface interface [26].

The railway locomotive running with initial velocity (v_o) is supposed to stand still with constant deceleration (a). Its linear translational velocity as function of time (t) is given by:

$$v(t) = v_0 - at \quad \text{---------- (3.1)}$$

$$\omega(t) = \frac{v(t)}{r(t)} \quad \text{---------- (3.2)}$$

$$\omega_{0=} = \frac{v(t)}{r_w} \quad \text{---------- (3.3)}$$

Where,

ω_o = Initial angular velocity the wheel

ω = angular velocity of the wheel at any time

v = velocity of the locomotive

v_o = Initial running velocity of the locomotive

r_w = the raus of locomotive wheel

During the application brake, the brake force acts at the effective radius (d_{isc}) of the disc rotor. The translational velocity (d_{isc}) of this frictional force (D_{isc}) could be expressed in terms of the translational velocity v (t) of the locomotive as follows.

$$v_{disc=} = v(t)\frac{r_{disc}}{r_w} \quad \text{---------- (3.4)}$$

The total braking time and distance can also be calculated by the formula:

$$S_b = t_b v_0 - \frac{a(t_b)^2}{2} \quad \text{---------- (3.5)}$$

$$t_{b=} = -\frac{v_0}{a} \quad \text{---------- (3.6)}$$

Hence, angular velocity (ω) at any time (t) could also be determined from:

$$\omega = \omega_0 - (1 - \frac{t}{t_b}) \quad (3.7)$$

Where,

t_b = brake time to stop the locomotive

S_b = total brake distance

Table 3.2 Data for Heat Flux Calculating

Item	Values
Mass of the vehicle – M [kg]	155,000
Start velocity – v_0 [m/s]	20
Deceleration – a [m/s^2]	1.2
Braking time – t_b [s]	15
Effective radius of the braking disc – r_d [m]	0.2475
Radius of the wheel – r_w [m]	0.625
Incline of the track – δ [‰]	11
Friction coefficient disc/pad – μ [/]	0.36
Surface of the braking pad A_p – [cm^2]	200

According to DIN EN ISO1183 the value μ = 0.36 of the friction coefficient for materials of the disc and the pad for locomotives is taken as the recommended value.

The specific loading condition under in this analysis is the downhill braking of the locomotive running with a maximum velocity of 72 km/hr to standstill with the temperature of the surrounding is 25°C. The assumed temperature is average environmental temperature of the operating route of the locomotive in the region.

3.2.2 Braking Energy of the Locomotive

During the process of braking, available energy of the locomotive that must be transformed into frictional heat, need to be determined accurately. This study considers the kinetic as well as the

potential (while running on slopes) energy of the locomotive that must be dissipated by the work of the braking. Rail vehicles have important masses in rotation. Therefore, the contribution of rotational kinetic energy is taken in to account. The initial kinetic energy imposed in to the locomotive is given by the sum total of translational and rotational.

$$E_K = \frac{1M(V_0)^2}{2} + \frac{1I(W_0)^2}{2} \quad \text{----------(3.8)}$$

Where,

E_k = Initial Kinetic Energy of the locomotive just before braking starts
M = Mass of the locomotive
I = Polar inertial moment of rotating parts

And, the moment of inertia of the rotating wheel set and discs can be calculated by using the equation below.

$$I = \sum_{i=1}^{n} m_i (r_i)^2 \quad \text{----------(3.9)}$$

Where,

m_i represents the masses of the wheel set and brake discs

r_i represents the rotation radius of the rotating parts from the center of rotation

For this case, all the rotating parts are fixed on the axle of the wheel set and the rotation axis could be taken as the tangent line joining the contact point of the rail heads with wheel set of the locomotive. It is the parallel to the axis of the wheel axle. Hence, the rotating radius is and equal to the radius of the wheel (r_w).Hence,

$$E_K = \frac{M(V_0)^2}{2} + \frac{I(W_0)^2}{2} = \frac{M(V_0)^2}{2}\left[1 + \frac{1}{M(r_w)^2}\right] = \frac{(1.1)M(V_0)^2}{2} \quad \text{----------(3.10)}$$

In Some literatures, the contribution of the rotating masses of the wheel set and discs is taken to be 10% the tare weight of the axle load of the locomotive. The term $[\frac{1}{M(r_w)^2}]$ accounts to the rotational masses involved and its value equals 0.1.The potential energy of the locomotive depends on the track gradient δ [mm/m] and on the travelled distance S_b [m].The exact definition of gradient is i=tan α where α is angle of inclination. According to EN 14531- 6, for calculation of external forces that result from gradients in railway applications, the Simplification sin α = tan α is commonly used. Therefore the potential energy is expressed as:

$$E_{P=}Mg\ {}_{b}\frac{\delta}{1000} \quad \text{---------- (3.11)}$$

Where, g = 9.81m/s^2

Therefore, the total available braking energy of the locomotive is determined from the equation below.

$$E_{b=}\frac{(1.1)M(V_0)^2}{2}+Mg\ {}_{b}\frac{\delta}{1000} \quad \text{---------- (3.12)}$$

3.2.3. Heat Energy

In braking system, the mechanical energy is transformed into heat energy. This energy is characterized by a total heating of the disc and the pads during the braking phase. The energy dissipated in the form of heat can generate rise in temperature ranging from 300^{O}C to 800^{O}C. The heat quantity in contact area is the result of plastic micro-deformation generated by the friction forces between disc rotor and brake pad. The total heat generated($Q_{gen)}$in the brake system equals with the total mechanical energy (Q_{gen}) lost from the locomotive. Hence, considering the energy balance;

$$E_{b=}Q_{gen} \quad \text{---------- (3.13)}$$

3.2.4. Work of Friction Force

When locomotive begins to brake, the train lost power and will stop by frictional forces. The imposed mechanical energy theoretically transformed to frictional heat. The brake disc rotor has got two friction surfaces ($2A_b$) swept by the brake pads on both sides. Two friction forces ($2F_{disc}$) act on both faces of the disc at an effective radius (r_{disc}). These forces retard the movement of the locomotive.

The total flux is equal to:

$$\text{Total heat flux}=\frac{Q_{gen}}{2A_b}=\frac{E_b}{2A_b} \quad \text{---------- (3.14)}$$

Where, A_b is the area swept by the brake pad at one face of the disc

S_{disc} = distance traveled by F_{disc} during the whole braking time

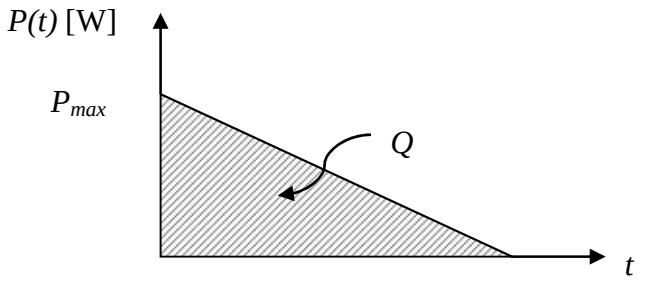

Figure 3.2 Heat input du t_b top braking

The total work of friction force during the whole brake cycle equals with the total heat generated.

$$Q_{gen} = E_{b=} \int_0^{t_b} p(t)dt \quad \text{---------- (3.15)}$$

$$\frac{(1.1)M(V_0)^2}{2} + MgS_b \frac{\delta}{1000} = \int_0^{t_b} p(t)dt$$

$$\frac{(1.1)M(V_0)^2}{2} + Mg\,S_b \frac{\delta}{1000} = 2F_{disc} \int_0^{t_b} v_{disc}(t)dt$$

$$\frac{(1.1)M(V_0)^2}{2} + Mg\,S_b \frac{\delta}{1000} = 2F_{disc}\frac{r_{disc}}{r_{wheel}}[t_b v_0 - \frac{a(t_b)^2}{2}])$$

The friction force that work on the disc to retard the locomotive is:

$$F_{disc} = \frac{\frac{(1.1)M(V_0)^2}{2} + MgS_b \frac{\delta}{1000}}{n_b 2(\frac{r_{disc}}{r_{wheel}} - [t_b v_0 - \frac{a(t_b)^2}{2}])} \quad \text{---------- (3.16)}$$

Where, n_b the number of disc brakes

In the present work, considering the amount of heat generation by wear is very small relative to the heat generated by friction, so the effect of material wear is neglected. Therefore, using the

Value of the frictional force obtained above, the transient heat flux can be determined. The heat Power generated at the effective radius (r_{disc}) of the disc can be expressed as:

$$Q'(t) = 2F_{disc}v_{disc} = 2F_{disc}\frac{r_{disc}}{r_{wheel}}(v_0 - \text{at}) \quad \text{---------- (3.17)}$$

3.2.5. Heat Flux Entering the Disc

The thermal analysis of the braking system of railway vehicles requires determination of the quantity of heat produced by friction, as well as the distribution of this energy between the railway disc and the braking pads. Generally, the thermal conductivity of material of the brake pads is smaller than that of disc ($k_p < k_d$). We consider the energy from brake application is converted into heat and transferred to the disc and pad approximately 95% and 5% respectively. This ratio normally is called the proportion of heat transferred to disc ($\gamma = 0.95$). The rate of heat generation is:

$$Q'd(t) = 2F_{disc}v_{disc} = .95F_{disc}\frac{r_{disc}}{r_{wheel}}(v_0 - \text{at}) \quad \text{---------- (3.18)}$$

$$Total\ heat\ flux = \frac{Q_{gen}}{2A_b} = \frac{E_b}{2A_b}$$

3.2.6. Centrifugal Force of the Disk

The disk rotating on the rail imposes the centrifugal force on its own due to its weight. Due to the centrifugal load the pressure/stress is applied to the surface of the disk width which is dependent on the density of the disk, rotational speed of the disk and the radius of the rotating disk. According to the UIC, S1002 and other railway standard the radius of the disk are selected to be 310 mm and density of high carbon cast iron, stainless steel, carbon/carbon composite and silicon carbide are 7150kg/m3, 7860kg/m3, 1750kg/m3 and 3100kg/m3 respectively and the rotational speed of the wheel is calculated from the speed of the vehicle in relation to the radius of the disk. Therefore the centrifugal force on the wheel is expressed as

$$F_c = r\rho_{disc}(W)^2 \quad \text{---------- (3.19)}$$

Where $F_{c\ is}$ the centrifugal force, ρ_b is density of the disk brake is the rotational speed of The disk and R is the radius of the disk. Since the maximum speed of train is 72Km/hr., the rotational speed of the disk is to be about 61.5rad/sec

3.2.7. Determination of Friction Surface of Disc

According to UIC 541-3 Standard, material brake pad and the four materials of Disc as shown in last discussion tables 5.1 to table 5.5, and with dimension tabulated in table 3.2 is used to Calculate friction area swept on the disc by the brake pad.

Table 3.3 Dimension of Disc and Brake Pad for Railway Locomotives

Description	Disc	Pad
Outer radius (R_o), [m]	0.31	0.31
Inner Radius (R_i)	0.175	0.24
Bolts hole and Radius	(ϕ13*9)	
Inner bore radius [m]	0.118	
Friction face Thickness (L)[m]	0.11	0.024
Effective friction radius (r_{disc})[m]	0.2475	-
Friction surface (A_b , A_P) [m_2]	0.2199	0.02

3.2.8. Determination of Heat Flux and Brake Disk Force

The value of the friction Force which work on the brake disc is calculated below by inserting the given values.

$$F_{disc} = \frac{\frac{(1.1)M(V_0)^2}{2x12} + MgS_b\frac{\delta}{1000}}{2(\frac{r_{disc}}{r_{wheel}} - [t_b v_0 - \frac{a(t_b)^2}{2}])} = 17499.72N$$

The Instant heat flux entering brake disc:

$$\frac{Q'(t)}{2A_b} = \frac{\gamma 2F_{disc}v_{disc}}{2A_b} = \frac{.95F_{disc}\frac{r_{disc}}{r_{wheel}}(v_0 - at)}{2A_b} = 749965.21 - 44997.91t\ (w)$$

3.2.9. Force (Surface Pressure) Determination for the Brake Caliper

The surface pressure between the disc and pad, on behave of the calculated force applied to the disc, needs to be determined. Hence, brake caliper pressure is:

$$p = \frac{F_{disc}}{\mu A_p} = \frac{17499.72}{.36x200x10\text{^} - 4} = 2.43[Mpa]$$

All the above calculated values are used throughout the finite element analysis.

3.3. PROCEDURE FOR FEM ANALYSIS WITH ANSYS

Static analysis is used to determine the displacements stresses, stains and forces in structures or components due to loads that do not induce significant inertia and damping effects. Steady loading in response conditions are assumed. The kinds of loading that can be applied in a static analysis include externally applied forces and pressures, steady state inertial forces such as gravity or rotational velocity imposed (non-zero) displacements, temperatures (for thermal strain).A static analysis can be either linear or non- linear. In our present work we consider linear static analysis. The procedure for static analysis consists of these main steps

- Building the model
- Obtaining the solution
- Reviewing the results

3.3.1. BUILD THE MODEL

In this step we specify the job name and analysis title use PREP7 to define the element types, element real constants, material properties and model geometry element type both linear and non- linear structural elements are allowed. The ANSYS elements library contains over 80 different element types. A unique number and prefix identify each element type.

E.g. BEAM 94, PLANE 71, SOLID 96 and PIPE 16

3.3.2. MATERIAL PROPERTIES

Young's modulus (ex) must be defined for static analysis. If we plan to apply inertia loads (such as gravity) we define mass properties such as density (DENS). Similarly if we plan to apply thermal loads (temperatures) we define coefficient of thermal expansion (ALPX).

3.3.3. SOLUTION STEPS ON FINITE ELEMENT ANALYSIS

In this step we define the analysis type and options, apply loads and initiate the finite element solution. This involves three phases:

- Pre-processor phase
- Solution phase
- Post-processor phase

Pre-processor

Pre-processor has been developed so that the same program is available on micro, mini, super-mini and mainframe computer system. This slows easy transfer of models one system to other.

Table 3.4. Shows the Brief Descriptions Steps Followed In Each Phase

Pre Preprocessor	Solution Phase	post-processor
Geometry definitions	Element matrix formulation	Post solution operations
Mesh generation	over all matrix triangulations	Post data print(for reports)
Material	Wave front	Post data
Definitions		Scanning post data display
Constraint definitions	Displacment,stress, etc	
Load definitions	Calculation	
Model display		

Pre-processor is an interactive model builder to prepare the FE (finite element) model and input data. The solution phase utilizes the input data developed by the pre-processor, and prepares the

solution according to the problem definition. It creates input files to the temperature etc. on the screen in the form of contours.

Geometrical Definitions:

There are four different geometric entities in pre- processor namely key points, lines, area and volumes. These entities can be used to obtain the geometric representation of the structure. All the entities are independent of other and have unique identification labels.

Model Generations:

Two different methods are used to generate a model:

- Direct generation.
- Solid modeling

With solid modeling we can describe the geometric boundaries of the model, establish controls over the size and desired shape of the elements and then instruct ANSYS program to generate all the nodes and elements automatically. By contrast, with the direct generation method, we determine the location of every node and size shape and connectivity of every element prior to defining these entities in the ANSYS model Although, some automatic data generation is possible (by using commands such as FILL, NGEN, EGEN etc) the direct generation method essentially a hands on numerical method that requires us to keep track of all the node numbers as we develop the finite element mesh. This detailed book keeping can become difficult for large models, giving scope for modeling error s. Solid modeling is usually more powerful and versatile than direct generation and is commonly preferred method of generating a model.

Mesh Generation:

In the finite element analysis the basic concept is to analyze the structure, which is an assemblage of discrete pieces called elements, which are connected, together at a finite number of points called nodes. Loading boundary conditions are then applied to these elements and nodes. A network of these elements is known as mesh.

Finite Element Generation

The maximum amount of time in a finite element analysis is spent on generating elements and nodal data. Preprocessor allows the user to generate nodes and elements automatically at the

same time allowing control over size and number of elements. There are various types of elements that can be mapped or generated on various geometric entities. The elements developed by various automatic element generation capabilities of pre-processor can be checked element characteristics that may need to be verified before the finite element analysis for connectivity, distortion-index etc., and automatic mesh generating capabilities of pre-processor are used rather than defining the nodes individually. If required nodes can be defined easily by defining the allocations or by translating the existing nodes. Also on one can plot, delete, or search nodes.

Boundary Conditions and Loading:

After completion of the finite element model it has to constrain and load has to be applied to the model. User can define constraints and loads in various ways. All constraints and loads are assigned set ID. This helps the user to keep track of load cases.

Model Display:

During the construction and verification stages of the model it may be necessary to view it from different angles. It is useful to rotate the model with respect to the global system and view it from different angles. Pre-processor offers this capability. By windowing feature pre-processor allows the user to enlarge a specific area of the model for clarity and details. Pre-processor also provides features like smoothness, scaling, regions, active set, etc. for efficient model viewing and editing.

Material Definitions:

All elements are defined by nodes, which have only their location defined. In the case of plate and shell elements there is no indication of thickness. This thickness can be given as element property. Property tables for a particular property set 1-D have to be input. Different types of elements have different properties for e.g. Beams: Cross sectional area, moment of inertia etc.

- Shell: Thickness
- Springs: Stiffness property. Property tables for a particular property set 1-D have to be input. Different types of elements have different properties for e.g. Beams: Cross sectional area, moment of inertia etc.
- Shell: Thickness
- Springs: Stiffness

- Solids: None

The user also needs to define material properties of the elements. For linear static analysis, modules of elasticity and Poisson's ratio need to be provided. For heat transfer coefficient of thermal expansion, densities etc. are required. They can be given to the elements by the material property set to 1-D

Solution:

The solution phase deals with the solution of the problem according to the problem definitions. All the tedious work of formulating and assembling of matrices are done by the computer and finally displacements and stress values are given as output. Some of the capabilities of the ANSYS are linear static analysis, non- linear static analysis, transient dynamic analysis, etc.

Post- Processor*:*

It is a powerful user- friendly post-processing program using interactive color graphics. It has extensive plotting features for displaying the results obtained from the finite element analysis.

One picture of the analysis results (i.e. The results in a visual form) can often reveal in seconds what would take an engineer hour to assess from a numerical output, say in tabular form. The engineer may also see the important aspects of the results that could be easily missed in a stack of numerical data. Employing state of art image enhancement techniques, facilities viewing of:

- Contours of stresses, displacements, temperatures, etc.
- Deform geometric plots
- Animated deformed shapes
- Time-history plots
- Solid sectioning
- Hidden line plot
- Light source shaded plot
- Boundary line plot etc.

The entire range of post processing options of different types of analysis can be accessed through the command/menu mode there by giving the user added flexibility and convenience

3.4. FINITE ELEMENT FORMULATION FOR HEAT CONDUCTION

The transient heat conduction of equation of each body for an axis-symmetric problem described in the cylindrical coordinate system is given as follow:-

$$Þc\frac{\partial T}{\partial t} = \frac{\partial}{\partial r}(K*r*\frac{\partial T}{\partial r}) + \frac{\partial}{\partial z}\left(k*\frac{\partial T}{\partial z}\right) - qv \quad ----------(3.20)$$

0 <= r <= R, 0 <= z <=

Where r-radial coordinate

Z-axial coordinates.

q_v- heat generation per volume

Where **r, c, k** are density, specific heat, and thermal conductivity of the material in r and z direction respectively

$$\frac{\partial T}{\partial z}(r,0,t) = \frac{\partial T}{\partial z}(r, L, t) = \frac{\partial T}{\partial z}(R,z,t) = h(T - T_{sur}), \frac{\partial T}{\partial r}(0,z,t) = 0$$

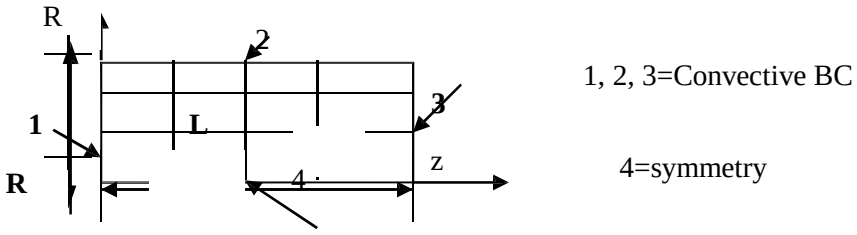

1, 2, 3=Convective BC

4=symmetry

Fig 3.3 boundaries conditions of transient heat

Where, h- convective heat transfer coefficient

T_{sur}-surrounding temperature

Initial condition:-

T(r, z, 0) =int.temp. Where int.temp.-initial temperature in degree Celsius over the domain.

FEM Analysis Procedures

The governing equation is

$$Þc\frac{\partial T}{\partial t} = \frac{1}{r}\frac{\partial}{\partial r}(K*r*\frac{\partial T}{\partial r}) + \frac{\partial}{\partial z}\left(k*\frac{\partial T}{\partial z}\right) \quad ----------(3.21)$$

In this specific problem there is no heat generation unit.

Applying Galerkin's method of weighted residual.

$$\int_{\Omega} Ni(r*c*Þ*\frac{\partial T}{\partial t}) - \frac{\partial}{\partial r}\left(k*r\frac{\partial T}{\partial r}\right) - r*\frac{\partial}{\partial z}(k\frac{\partial T}{\partial z}))d\Omega = 0 \quad ----------(3.22)$$

Where: - Ni-weight function equal to interpolating function

T-trial function

Integrating by parts results in

$$\int_{\Omega} Ni(r*c*Þ*\frac{\partial T}{\partial t})d\Omega + \int_{\Omega}(k*r\frac{\partial Ni}{\partial z}\frac{\partial T}{\partial z})d\Omega - \int_{r}(k*r\frac{\partial T}{\partial n})d\Gamma = 0 \quad --------(3.23)$$

Discretizing system domain

In this particular case the system domain is discretized in to rectangular ring elements

Expressing the trial function and its derivatives in terms of the shape functions &nodal values.

$$\sum_{j=1}^{nnel} NjTj, \quad \frac{\partial T}{\partial r} = \sum_{j=1}^{nnel}\frac{\partial Nj}{\partial r}Tj, \frac{\partial T}{\partial z} = \sum_{j=1}^{nnel}\frac{\partial Nj}{\partial z}Tj, \frac{\partial T}{\partial t} = \sum_{j=1}^{nnel}\frac{Ni\partial T}{\partial t} \quad ------(3.24)$$

$$\int_{\Omega} Ni*r(Þ*C*Nj\frac{\partial T}{\partial t})d\Omega + \int_{\Omega}(k*r\sum_{j=1}^{nnel}\frac{\partial Nj}{\partial r}Tj + k*r*\frac{\partial Nj}{\partial z}$$

$$=> \sum_{j=1}^{nnel}(\frac{\partial Nj}{\partial r}Tj)d\Omega - \int_{r}(k*r\frac{\partial T}{\partial n})d\Gamma = 0 \quad ----------(3.25)$$

Substitute the above equation into the weak integral form.

Where-nnel-number of nodes per element. (nnel=4)

Defining element equation

$$[C]^e\left\{\frac{\partial T}{\partial t}\right\} + [K]^e\{T\} = \{f\}^e \quad ----------(3.26)$$

$$Where\ [\mathrm{K}] = \int_{\Omega}(k * r * \frac{\partial Ni}{\partial r}\sum_{j=1}^{nnel}\frac{\partial Nj}{\partial r} + k * r * \frac{\partial Ni}{\partial z}\sum_{j=1}^{nnel}\frac{\partial Nj}{\partial r})d\Omega$$

i=1: nnel.

$$\{\mathrm{T}\} = [\mathrm{T1}, \mathrm{T2}, \mathrm{T3}, \mathrm{T4}]^{\mathrm{T}}.$$

$$[\mathrm{C}]^{e} = \int_{\Omega} Ni * r * Þ * C * Nj\, d\Omega$$

$$\{\mathrm{f}\}^{e} = \int_{r}(k * r\frac{\partial T}{\partial n})d\Gamma$$

Where h-convective heat transfer coefficient.

T_{sur} −Surrounding temperature

$$and\ kn * \frac{\partial T}{\partial n} = -q\ (\mathrm{w/m^2})\ \ for\ prescribed\ boundary\ condition$$

The equation can be modified as

$$\{\mathrm{f}\} = \int_{r} r * h * Ni * T_{sur}\, d\Gamma - \int_{r} r * Ni * (q)^{-} d\Gamma - (3.27)$$

$$K = \int_{\Omega}(k * r * \frac{\partial Ni}{\partial r}\sum_{j=1}^{nnel}\frac{\partial Nj}{\partial r} + k * r * \frac{\partial Ni}{\partial z}\sum_{j=1}^{nnel}\frac{\partial Nj}{\partial r})d\Omega + \int_{r} r * h * Ni * \sum_{j=1}^{nnel} Nj d\Omega - - (3.28)$$

i=1: nnel.

Numerical Integration

Using isoperimetric bilinear rectangular elements, the shape functions are defined in the normalized natural coordinates *and* .

2x2 points Gauss-Quadrature Numerical integration is performed to develop the element capacitance, stiffness Matrix, and load vector.

The radius is taken at the points of integration.

Assembly of element equation to system equation and Imposition of boundary condition.

$$[\mathrm{C}]^{e}\left\{\frac{\partial T}{\partial t}\right\} + [\mathrm{K}]^{e}\{T\} = \{\mathrm{f}\}^{e} - (3.29)$$

Time Marching or Integration.

In this case the generalized Θ-method is adapted

$$([\mathrm{C}] + \Theta * \mathrm{dt} * [\mathrm{K}])\{\mathrm{T}\}^{n+1} = dt\{\mathrm{F}\}^{n} + ([\mathrm{C}] - (1-\Theta) * \mathrm{dt} * [\mathrm{K}])\{\mathrm{T}\}^{n} - - - - - - - - (3.30)$$

Where dt-time step size.

For Explicit (forward difference) method Θ**=0.**

For full Implicit (backward difference) method Θ**=1.**

For Crank-Nicolson method Θ=**0.5**.

For Galerkin method Θ=**2/3**.

For different value of **Θ,** the well-known numerical integration scheme can be obtained in this study, 0.5 <or = Θ >or =1.0 was used, which is numerically stable scheme.

3.5. THERMAL ANALYSIS

A thermal analysis calculates the temperature distribution and related thermal quantities in brake disk. Typical thermal quantities are:

- The temperature distribution
- The amount of heat lost or gained

- . Thermal fluxes. types of thermal analysis determines the temperatureDistribution and other thermal quantities under steady state loading Conditions. A steady state loading condition is a situation where Heat storage effects varying over a period of time can be ignored. A transient thermal analysis determines the temperature distribution

And other thermal quantities under c o n d i t i o n s that varying over a period of time. Planning the analysis: In this step a compromise between the computer time and accuracy of the analysis is made. The various parameters set in analysis are given below: Thermal modeling.

- Analysis type! Thermal h-method.
- Steady state or Transient? Transient
- Thermal or Structural? Thermal
- Properties of the material? Isotropic
- Objective of analysis- to find out the temperature distribution in the brake disk when the process of braking is done.
- Units- SI

3.6. STRUCTURAL ANALYSIS

Structural analysis is the most common application of the finite element analysis. The term

structural implies civil engineering structure such as bridge and building, but also naval, aeronautical and mechanical structure such as ship hulls, aircraft bodies and machine housing as well as mechanical components such as piston, machine parts and tools.

Types of Structural Analysis:

The seven types of structural analyses in ANSYS. One can perform the following types of structural analysis. Each of these analysis types are discussed as follows:

- Static analysis
- Modal analysis
- Harmonic analysis
- Transient dynamic analysis
- Spectrum analysis
- Buckling analysis
- Explicit dynamic analysis

Structural static analysis

A static analysis calculates the effect of steady loading conditions on a structure,while ignoring the ineritia and damping effects such as thosecaused by time varing loads. A static analysis can,however include steady ineritia loads(such as a gravity and rotational velocity) and time varing loads that can be approximated as static equivalent loads (such as static equivalent wind and seismic loads)

CHAPTER 4:

MODELING AND ANALYSIS

It is very difficult to exactly model the brake disk, in which there are still researches are going on to find out transient thermo elastic behavior of disk brake during braking applications . There is always a need of some assumptions to model any complex geometry. These assumptions are made, keeping in mind the difficulties involved in the theoretical calculation and the importance of the parameters that are taken and those which are ignored. In modeling we always ignore the things that are of less importance and have little impact on the analysis. The assumptions are always made depending upon the details and accuracy required in modeling.

The assumptions which are made while modeling the process are given below:-

- The disk material is considered as homogeneous and isotropic.
- The domain is considered as axis- symmetric.
- The disk is stress free before the application of brake.
- Brakes are applied on the entire six wheels.
- The analysis is based on pure thermal loading and vibration and thus only stress level due to the above said is done. The analysis does not determine the life of the disk brake.
- Only ambient air-cooling is taken into account and no forced Convection is taken
- The kinetic, rotational and potential energy of the locomotive is lost through the brake disks i.e. No heat loss between the tire and the road surface and deceleration is uniform.
- The disk brake model used is of solid type and not ventilated one.
- The thermal conductivity of the material used for the analysis is Uniform throughout.
- The specific heat of the material used is constant throughout and does not change with temperature.
- The heat transfer coefficient h is constant during simulation of braking process.
- Radiation is neglected by virtue of short braking time and hence relatively low temperature;

4.1. DEFINITION OF PROBLEM DOMAIN

Due to the application of brakes on the locomotive disk brake rotor , heat generation takes place due to friction and this thermal flux has to be conducted and dispersed across the disk rotor cross section. The condition of braking is very much severe and thus the thermal analysis has to be carried out. The thermal loading as well as structure is axis -symmetric. Hence axis-symmetric analysis can be per formed, but in this study we performed 3-D analysis, which is an exact representation for this thermal analysis. Thermal analysis is carried out and with the above load structural analysis is also performed for analyzing the stability of the structure.

4.2. CREATING A FINITE ELEMENT MESH

According to given specifications the element type chosen is solid 90.Solid 90 is higher order version of the 3-D eight node thermal element (Solid 70). The element has 20 nodes with single degree of freedom, temperature, at each node. The 20-node elements have compatible temperature shape and are well suited to model curved boundaries. The 20-node thermal element is applicable to a 3-D dimensional transient thermal analysis. If the model containing this element is also to be analyzed structurally, the element should be replaced by the equivalent structural element (Solid 95).

Fitting mechanism of solid disc into axle

The solid discs have to be fitted over the axle by the process of fitting and the hub bore should provide a press fit.

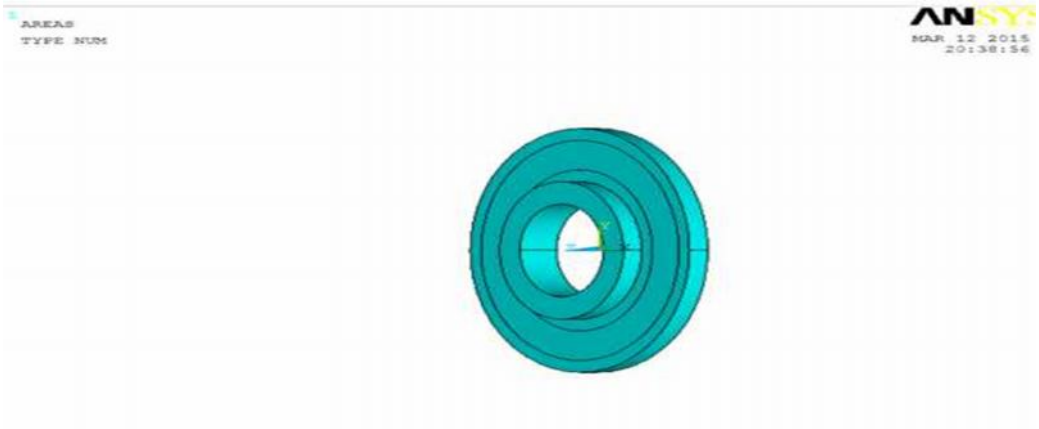

Figure. 4.1. Model of 30 Mm Solid Disk Brake

4.3. SOLID90 ELEMENT GEOMETRY

The geometry, node locations, and the coordinate system for this element are defined by 20-node points and the material properties. A prism- shaped element may be formed by defining duplicate K, L, and S; A and B, and O, P, and W node numbers. A tetrahedral-shaped element and a pyramid-shaped element may also be formed .Element loads are described in node and element loads. Convection or heat flux (but not both) and radiation may be input as surface loads at the element faces. Heat generation rates may be input as element body loads at the nodes. If the node I heat generation rate HG (I) is input, and all others are unspecified, they default to HG (I). If all corner node heat generation rates are specified each mid side node heat generation rate defaults to the average heat generation rate of its adjacent corner nodes.

SOLID90 Input Summary

- Nodes I, J, K, L, M, N, O, P, Q, R, S, T, U, V, W, X, Y, Z, A, B
- Degrees of Freedom T e m p e r a t u r e
- Real Constants None
- Material Properties KXX, KYY, KZZ, DENS, C, ENTH
- Surface Loads Convection or Heat Flux (but not both) and Radiation

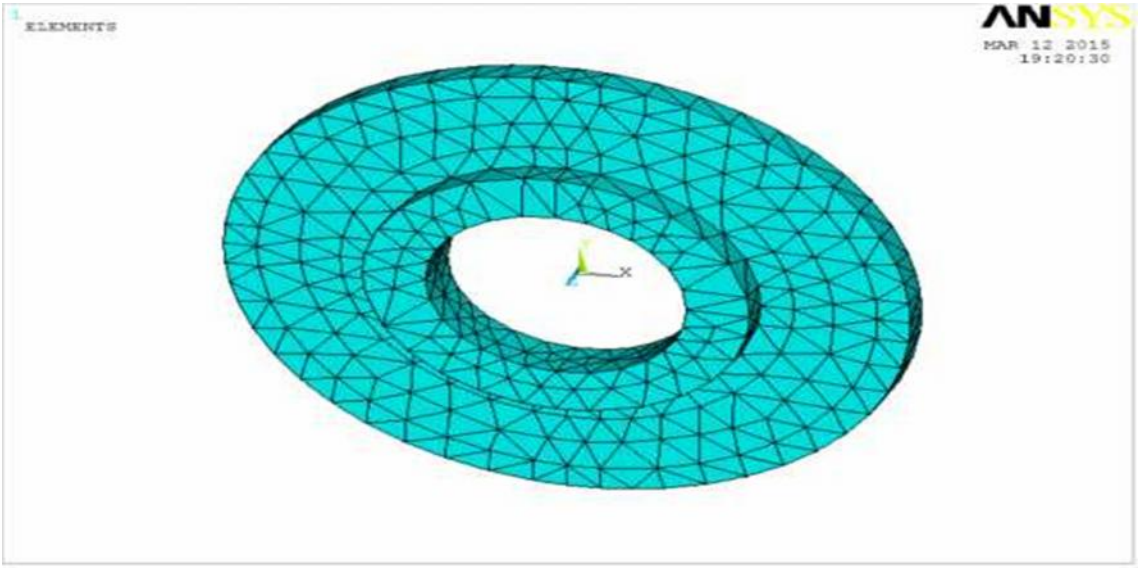

Figure 4.2 3-D Solid Disk Meshed Model

4.4. APPLYING THE BOUNDARY CONDITIONS

In thermal and structural analysis of disk brake, we have to apply thermal and boundary conditions on 3-D disk model of solid disk brake.

4.4.1. THERMAL BOUNDARY CONDITIONS

As shown in Fig. 4.3 a model presents a three dimensional solid disk squeezed by two finite-width friction material called pads. The entire surface, S, of the disk has three different regions including S1 and S2. On S1 through circular area heat flux is specified due to the frictional heating between the pads and disk, and S2 is defined for the convection boundary. The rest of the region, except S1 U S2, is either temperature specified or assumed to be insulated: the inner and outer rim area of disk.

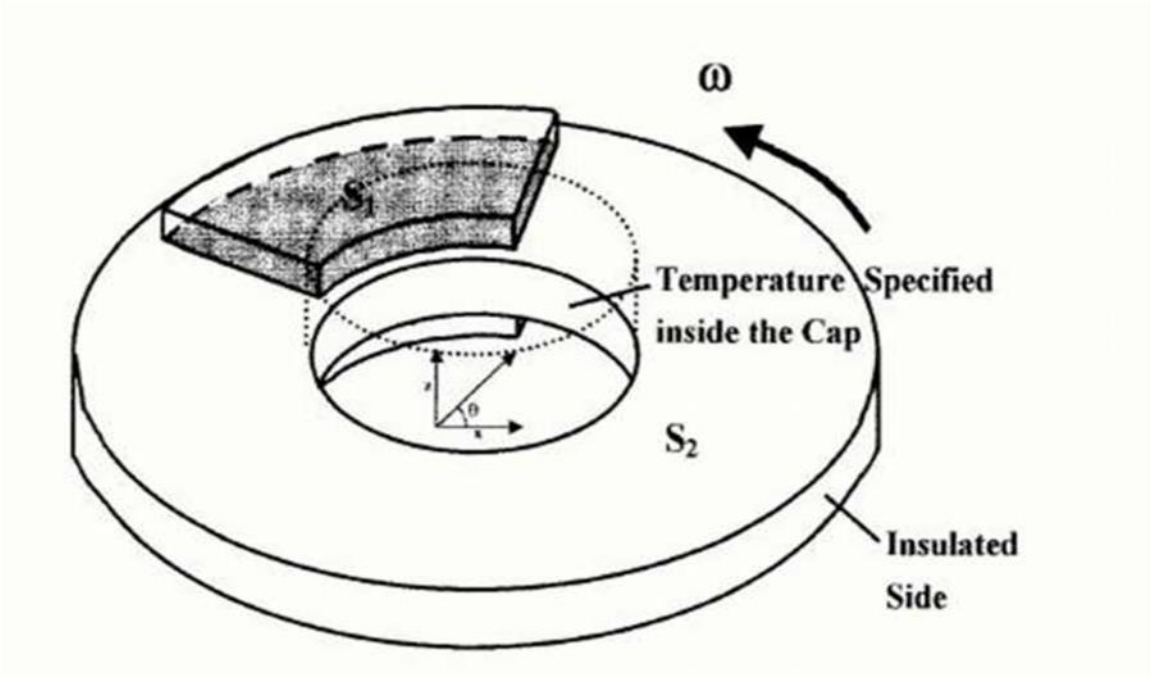

Figure 4.3 Thermal Model of Solid Disk Brake

In the contact region S1, the local shear traction cause frictional heating that flows into the disk and pads. Heat flux q on a contact area is updated per the pressure distribution at every simulation step

4.4.2. STRUCTURAL BOUNDARY CONDITIONS

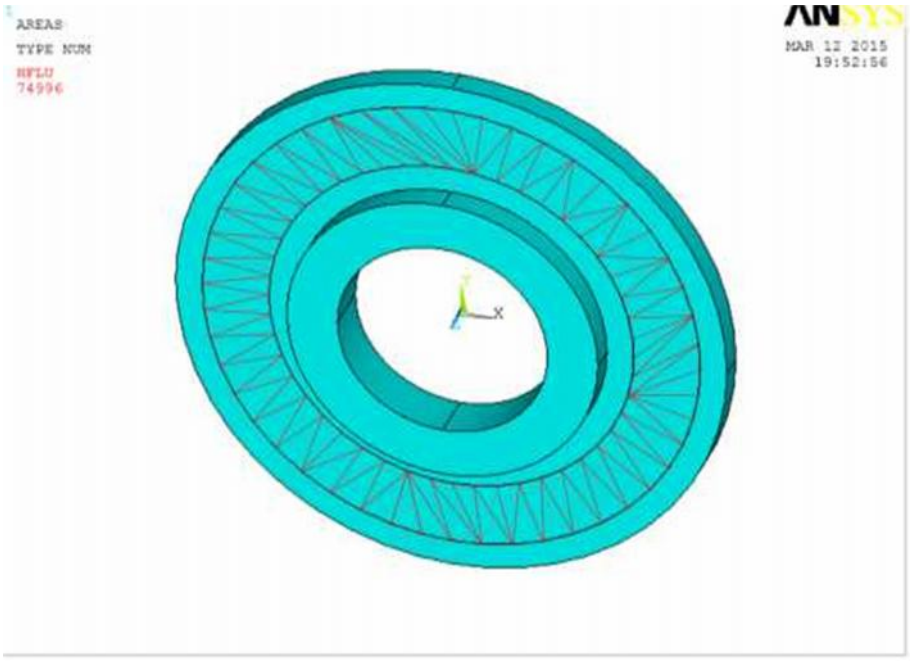

Figure 4.4 Structural Model of Solid Disk Brake

4.5. SOLUTION DESCRIPTION IN DETAIL ON MODELING AND ANALYSIS

In the solution procedure, frontal solver is used. It involves after the individual element matrices are calculated, the solver reads in the degree of freedom (DOF) for the first element. The program eliminates any degrees of freedom that can be expressed in terms of the other DOF by writing an equation to the .tri file. This process repeats for all the elements until all the degree of freedom have been eliminated and a complete triangular zed matrix is left on the .tri file. The term frequently used is the frontal solver is wave front. The wave front is the number of degrees of freedom retained by the solver while triangularization of the matrix. The nodal solution plot of temperature distribution in thermal analysis. Graph of the temperature variation with respect to the radial distance from the point of application of the heat flux. Graph of the temperature variation with respect to the time. The nodal solution plot of stress distribution in structural analysis

CHAPTER 5:

RESULTS AND DISCUSSIONS

5.1 Candidate Materials Property for the Disc Brake Rotor

Two very different vehicle brake tests are often simulated to critically examine maximum temperatures and integrity of new rotor materials and designs for the following candidate materials

–along slope decent during which the brakes are dragged

- A repeated high speed stop with the rotor allowed cooling only moderately between stops

They former test determines the capable of heat transfer to the atmosphere during repeated stop, The ability of the material to with stand repeated thermal cycling, And the ability of the friction pair to resist fade under these severe conditions.

5.2. Validation of Results

First of all, to validate the present method, a comparison of transient results with four different materials and different braking steps of time solution of thermo elastic behaviors was performed for the operation condition of the calculated heat flux .(drag brake application) during 16 seconds that is 4^{th},8^{th},12^{th} and 16^{th} sec as shown in the following figures the transient solution for this operation condition of the temperature and thermal vector flux sum increases symmetrically axis at the contact areas, then converges to the end of the disc to lower the temperature and thermal heat flux as sown in figures 5.1 to 5.14 , it can be regarded as validation of the applied transient scheme. The thermal boundary condition assumptions are adiabatic on The boundary of the inner and outer radius. The prescribed temperature condition (i.e. ambient temperature T= 20℃) on both boundaries along the radius of the lower and upper pad by Assumption of the cooling state. The four braking steps, material properties and operation

conditions used for the validation of the transient thermo elastic scheme are given in the following tables. The time described in the table form Step Δt=0.5sec was used. Fig 5.1 shows the thermal heat flux vector distribution on the friction surfaces for the transient case (at t=8 sec) solution. Actually, after time t=4 sec, a change of heat flux distribution does scarcely

occur, and then the steady state is reached. Correspondingly, this result indicates that the heat flux distribution on each friction surface occur dissimilarly as time elapse. The major cause of these phenomena is that the contact condition on the friction surfaces is changed to satisfy the new equilibrium state due to the rise in temperature. Fig 5.2 presents the temperature distributions on the friction surfaces for the transient (at t=8 sec) results. As the preceding results, the trend is for the temperature distribution to converge towards at the end of the two radius of the disc.

Validation Of Results

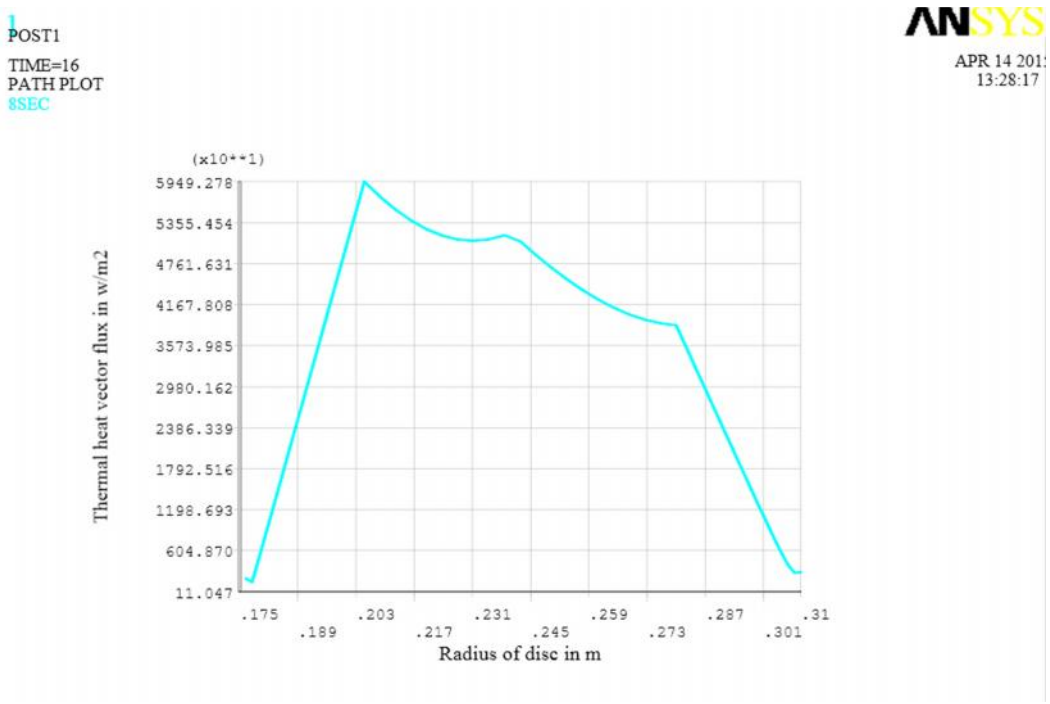

Figure 5.1 Heat Flux Distribution of Disc Brake Radius on Friction Surfaces during 8thsec Braking Step

5.3. Thermo Elastic Behavior in Contact between Pad and Disc Radius of Brake Application in Four Materials

To investigate the transient thermo elastic analysis behavior of the four materials' of disc brake, the ANSYS simulation is obtained in 16 repeated brake applications using the method general post-processor by reading results to show graph results of different materials properties that is pad, disc and hub materials are actually considered into ANSYS per-processor materials properties as shown table 5.1to table 5.5. The input materials, the time history

load step value is same and at end of load step 300sec time stepped size is 4sec, the results shows that in every contact areas are different values at contact area initially it was small values a few second. The temperature and thermal heat vector flux increases in a manner of symmetrically axis to maximum in pad and disc contact area then decreases at the end of disc and in the hub (axle) area.The heat convection coefficient for the four materials are considered by thermodynamic assumption taken as h=100(w/m^2k).

In my project from thermodynamic consideration h is considered as =50-100 (w/m^2k). And i have considered for the four candidate materials and also h is depending on air property not the materials property, I have taken the maximum value from the range mentioned these is my assumption.

Table 5.1 Material Property of High Carbon Cast Iron

Materials Properties	**Pad**	**Disk**	**Axle(hub)**
Thermal Conductivity, k(w/mk)	5	50	51.9
Density, Þ(kg/ M3)	1400	7150	7872
Specific Heat ,c(j/kgk)	1000	438	481
Poisons Ratio,v	0.25	0.29	0.29
Thermal Expansion,α(10-6/k)	10	10	12.6
Elastic Modulus, E(Gpa)	1	83	205

Table 5.2 Material Property of Stainless Steel

Materials Properties	**Pad**	**Disk**	**Axle(Hub)**
Thermal Conductivity, K(W/Mk)	5	16.2	51.9
Density, Þ(Kg/ M3)	1400	7860	7872
Specific Heat ,C(J/Kgk)	1000	500	481
Poisons Ratio,V	0.25	0.25	0.29
Thermal Expansion(10-6/K)	10	17.2	12.6
Elastic Modulus, E(Gpa)	1	193	205

Table 5.3 Material Property of Carbon/Carbon Composite

Materials Properties	Pad	Disk	Axle(Hub)
Thermal Conductivity, k(w/mk)	5	95	51.9
Density, Þ(kg/ M3)	1400	1750	7872
Specific Heat ,c(j/kgk)	1000	1000	481
Poisons Ratio,v	0.25	0.17	0.29
Thermal Expansion(10-6/k)	10	0.7	12.6
Elastic Modulus, E(Gpa)	1	40	205

Table 5.4 Material Property of Silicon Carbide

Materials Properties	Pad	Disk	Axle(hub)
ThermalConductivity, K(W/Mk)	5	125.6	51.9
Density, Þ(Kg/ M3)	1400	3100	7872
Specific Heat ,C(J/Kgk)	1000	670	481
Poisons Ratio,V	0.25	0.14	0.29
Thermal Expansion(10-6/K)	10	4	12.6
Elastic Modulus, E(Gpa)	1	410	205

Validation of results

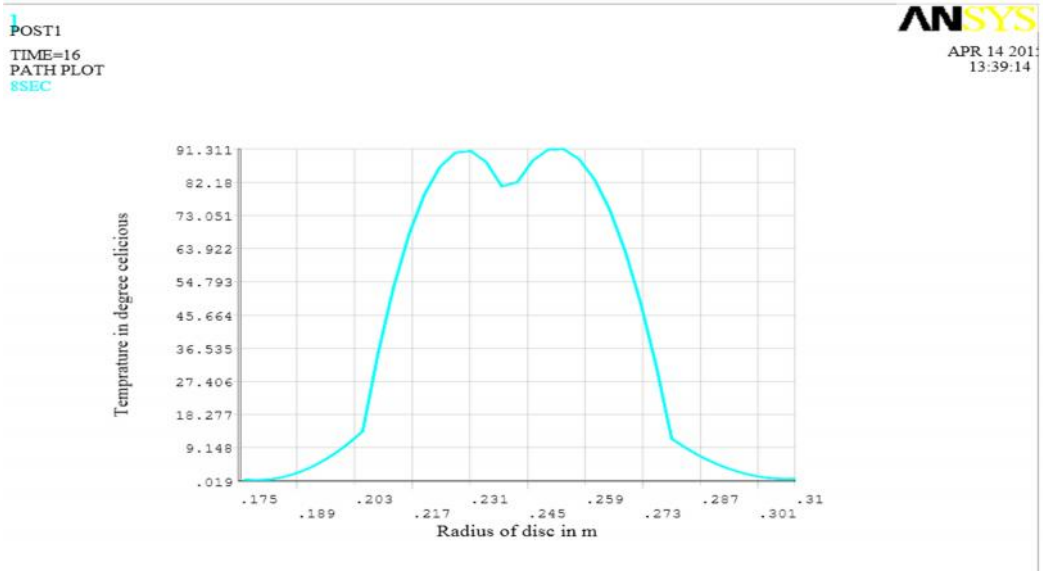

Figure 5.2. Temperature Distribution of Disc Brake Radius on Friction Surfaces during 8thsec Braking Step

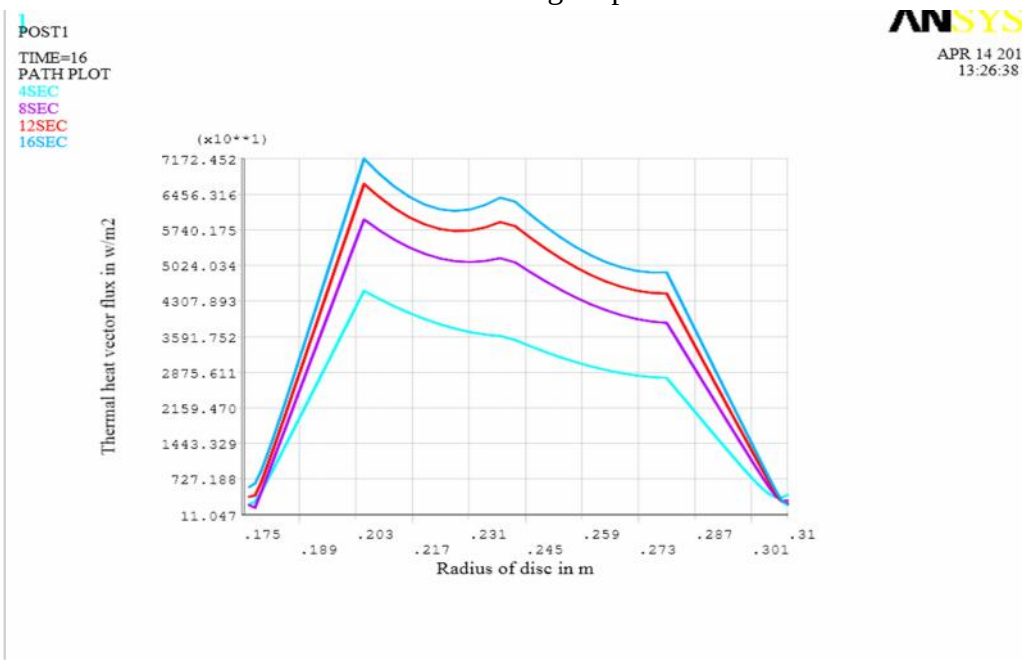

Figure 5.3 Heat Flux Distributions of 30 mm High Carbon Cast Iron Disk Radius on Friction Surfaces of Disk Brake in Various Braking Step

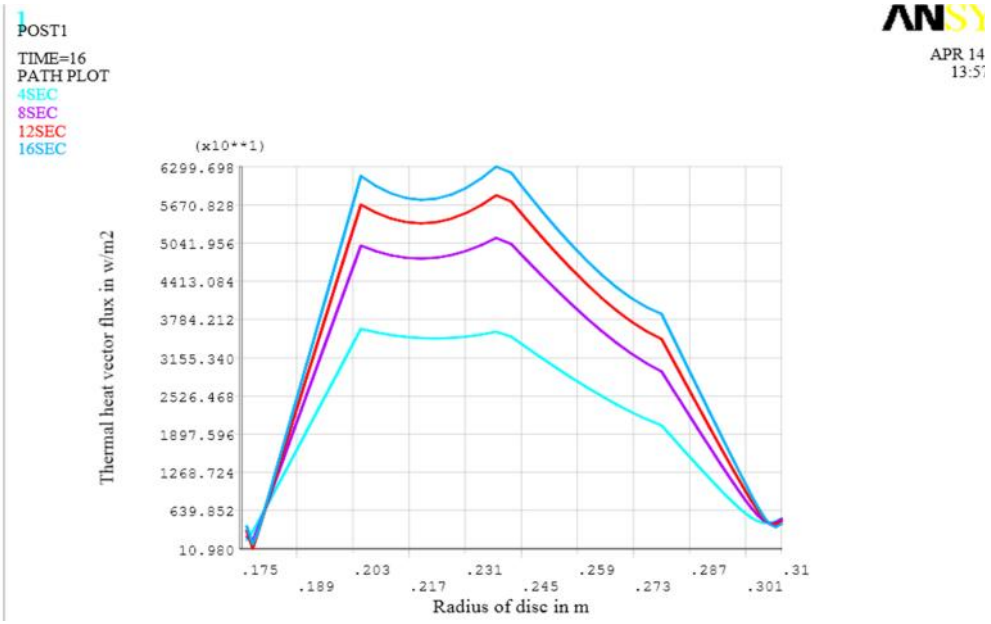

Figure 5.4 Heat Flux Distributions of 30 mm Stainless Steel Disk Radius on Friction Surfaces in Various Braking Step

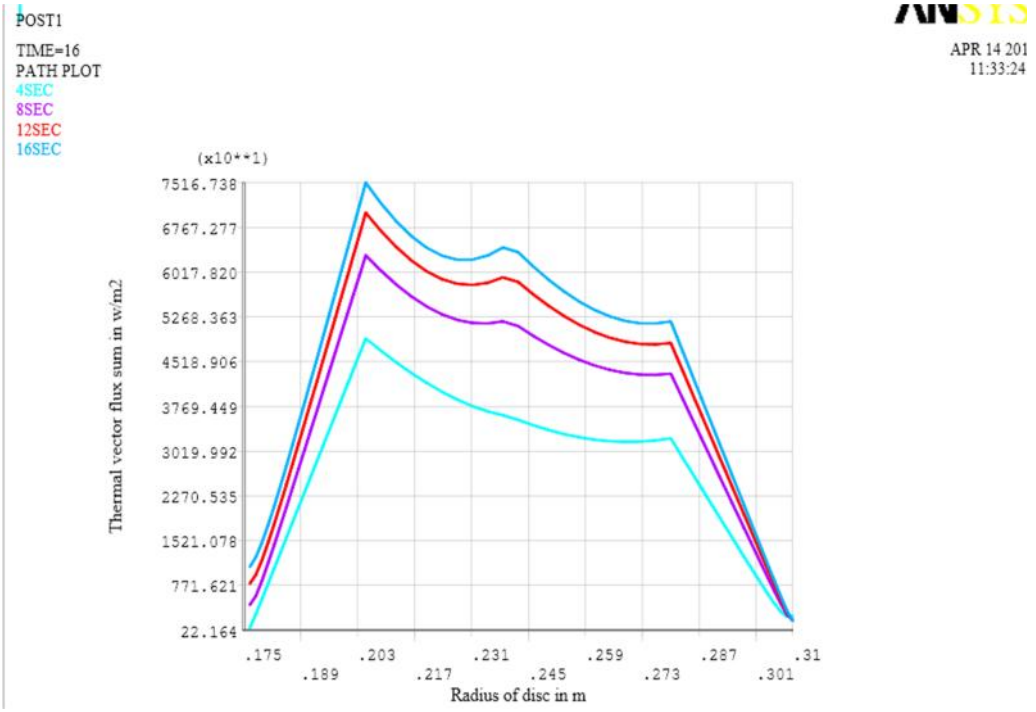

Figure 5.5 Heat Flux Distributions of 30 mm Carbon/Carbon Composite Disk Radius On Friction Surfaces in Various Braking Step

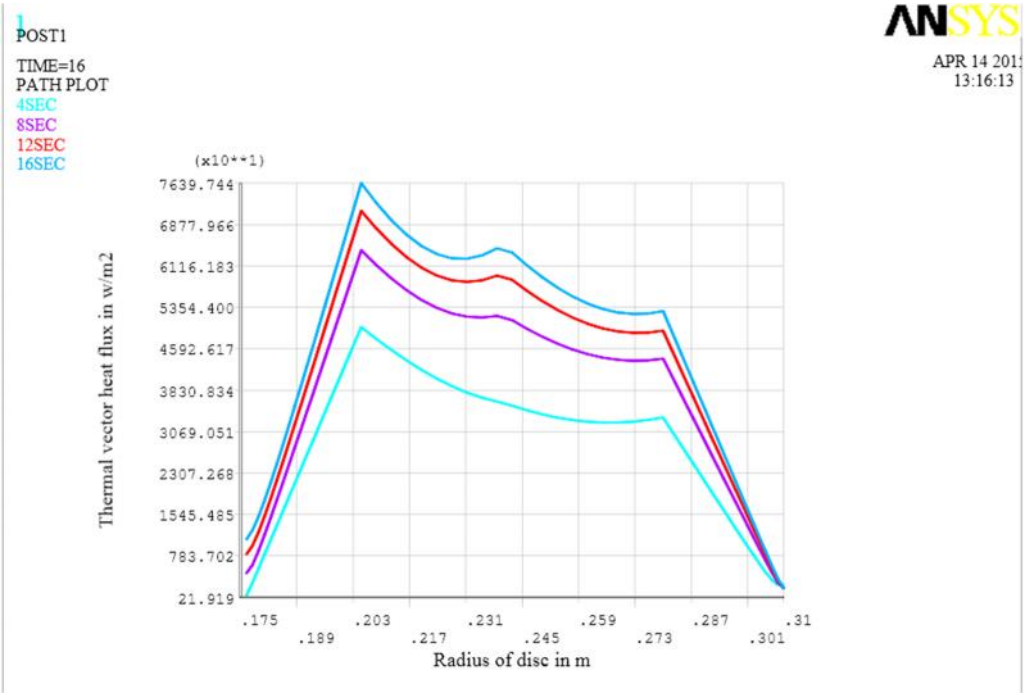

Figure 5.6 Heat Flux Distributions of 30 mm Silicon Carbide Disk Radius on Friction Surfaces in Various Braking Step

In addition to the TEI phenomenon of disk brakes, the influence of the material properties of the pad on the contact ratio of friction surfaces is considered to facilitate better conceptual design of the disk brake system. Fig 5.7 to Fig 5.10 showed the effect of material properties in a thermo elastic contact stability problem with one body in contact with a rigid plane surface. However, the present results in Fig 5.7, Fig 5.8 , Fig 5.9 and fig 5.10 are further show the relative importance of each parameter on the variation of thermo elastic behaviors. The thermal expansion coefficient and the elastic modulus of pad and disk materials have a larger effect on the thermo elastic behaviors of disk brakes. In particular, when the elastic modulus of pad material is halved, all friction surfaces between the disk and pad are in perfect contact for all of the braking steps. Therefore, the softer pad improves the contact pressure distribution and results in a more even temperature distribution.

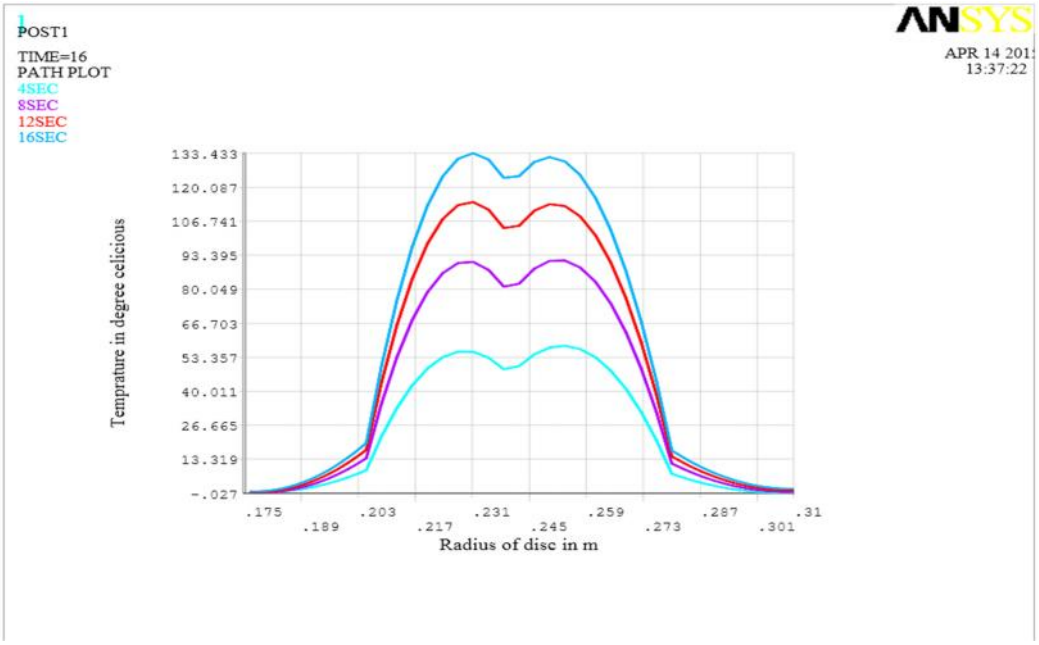

Figure 5.7 Temperature Distributions of 30 mm High Carbon Cast Iron Disk Radius On Friction Surfaces in Various Braking Step

Also, similar analyses were carried to investigate the effects of disc material properties. It was found that the thermal expansion coefficient and the specific heat of disk materials have a larger influence on the thermo elastic behaviors. Based on these numerical results, the thermo elastic behaviors of the four disk brake materials are also investigated those are; Carbon composites, high carbon cast iron, silicon carbide and stainless steel are extensively used as aircraft disk brakes, rocket re-entry nose tips, and high speed railway brakes on account of their excellent material properties (high temperature resistance, low density, high thermal conductivity and heat capacity, and low thermal expansion). In this section, the transient thermo elastic analysis of the high carbon cast iron disk brake is performed for the drag brake application for 16sec and then the results in the case of high carbon cast iron (orthotropic case) are compared with those using the material properties listed in Table 5.2(isotropic case). The materials properties of high carbon cast iron used in the computations are presented in Table 5.5.

Table 5.5. Isentropic, High Carbon Cast Iron

Materials Properties	**Pad and Disk**
Thermal Conductivity, k(w/mk)	50
Density, Þ(kg/ M3)	1800
Specific Heat ,c(j/kgk)	1420
Poisons Ratio,v	0.3
Thermal Expansion,α(10-6/k)	0.3
Elastic Modulus, E(Gpa)	50.2

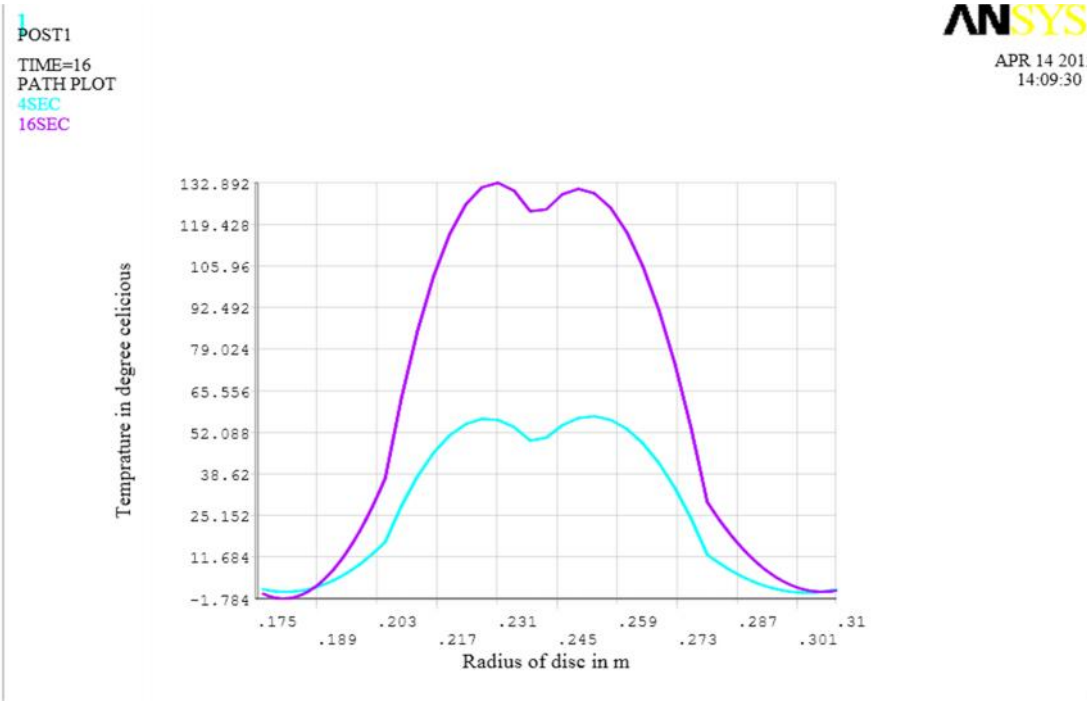

Figure 5.8. Temperature Distribution of 30 mm Stainless Steel Disk Radius on Friction Surfaces in Various Braking Step

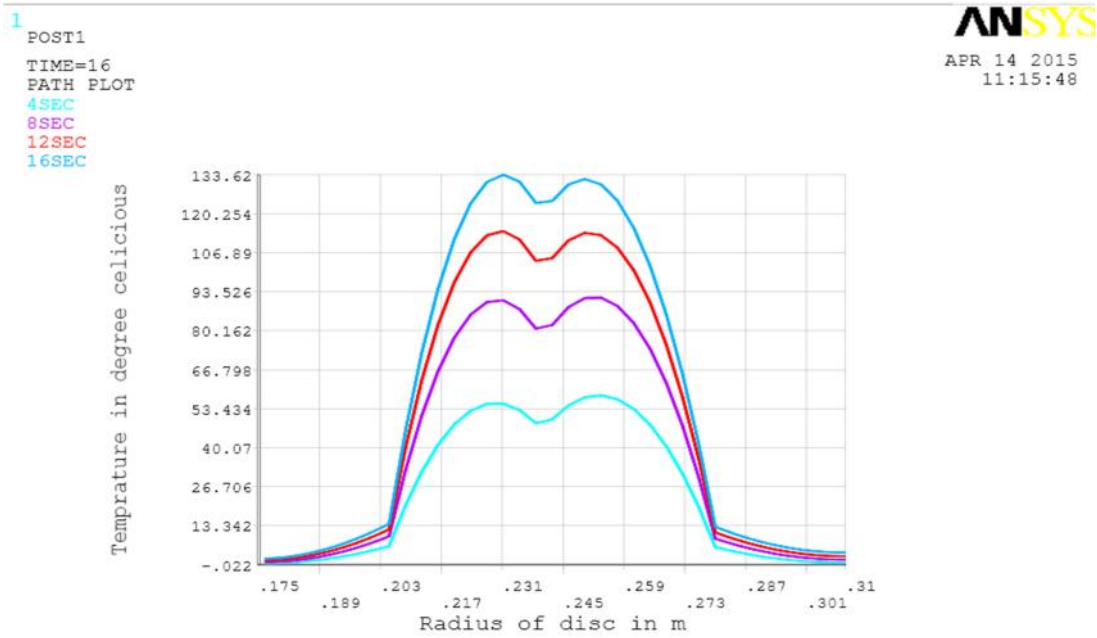

Figure 5.9. Temperature Distribution of 30 mm Carbon/Carbon Composite Disk Radius on Friction Surfaces in Various Braking Step

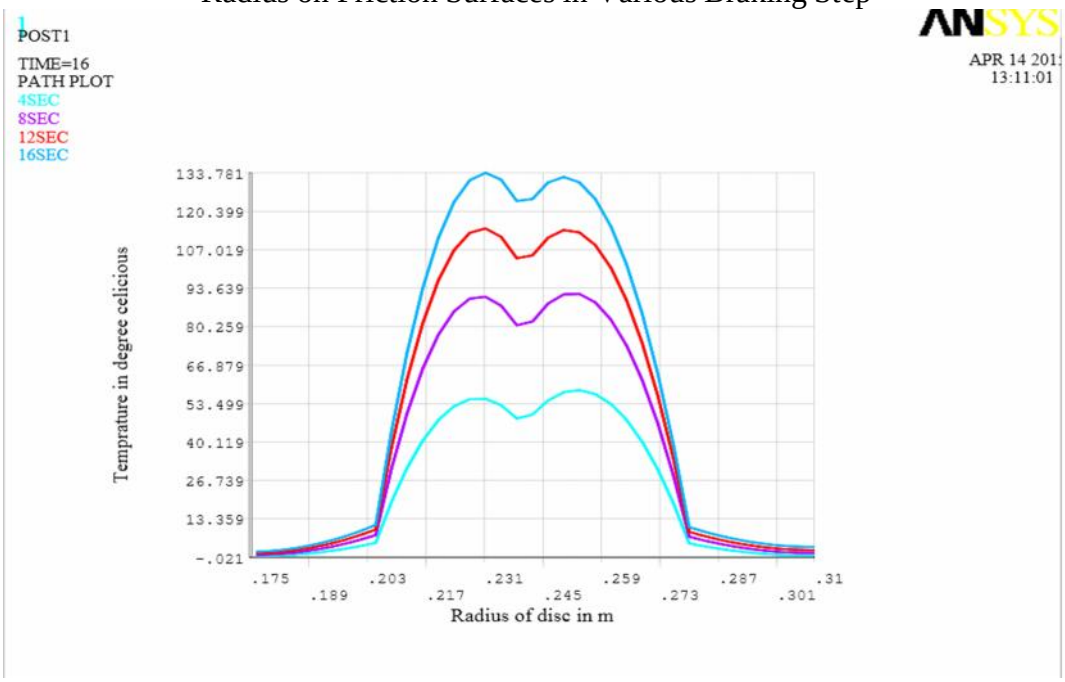

Figure 5.10 Temperature Distributions of 30 mm Silicon Carbide Disk Radius on Friction Surfaces in Various Braking Step

Figure 5.11, 5.12, 5.13 and 5.14 show the heat flux and temperature distributions on the friction surfaces material of high carbon cast iron at time=4s and 16 s for the isotropic and orthotropic material respectively. Compared with the isotropic case, the heat flux of the

orthotropic one are very uniformly distributed along the friction surfaces and results in a more even temperature distribution, namely, a thermo elastic stable state. These results show that the disk brakes made of orthotropic material can provide better braking performance than the isentropic metal ones.

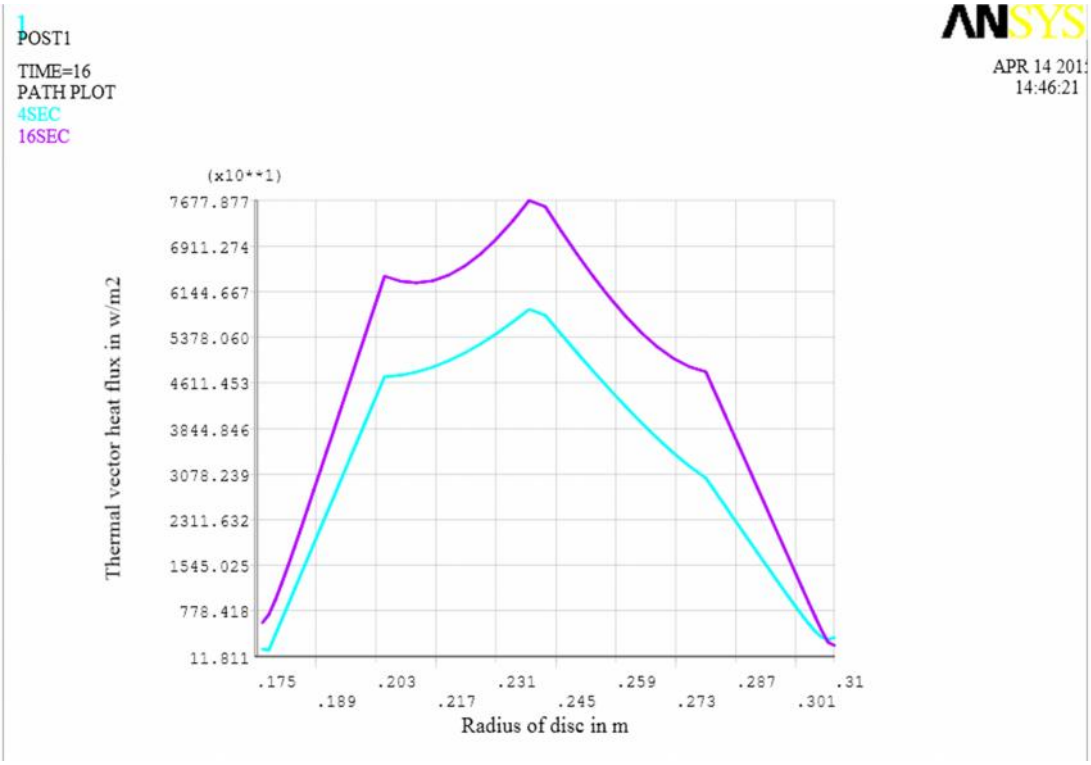

Figure 5.11. Heat Flux Distribution of Isentropic 30 mm High Carbon Cast Iron Disk Radius on Friction Surfaces in Two Braking Step

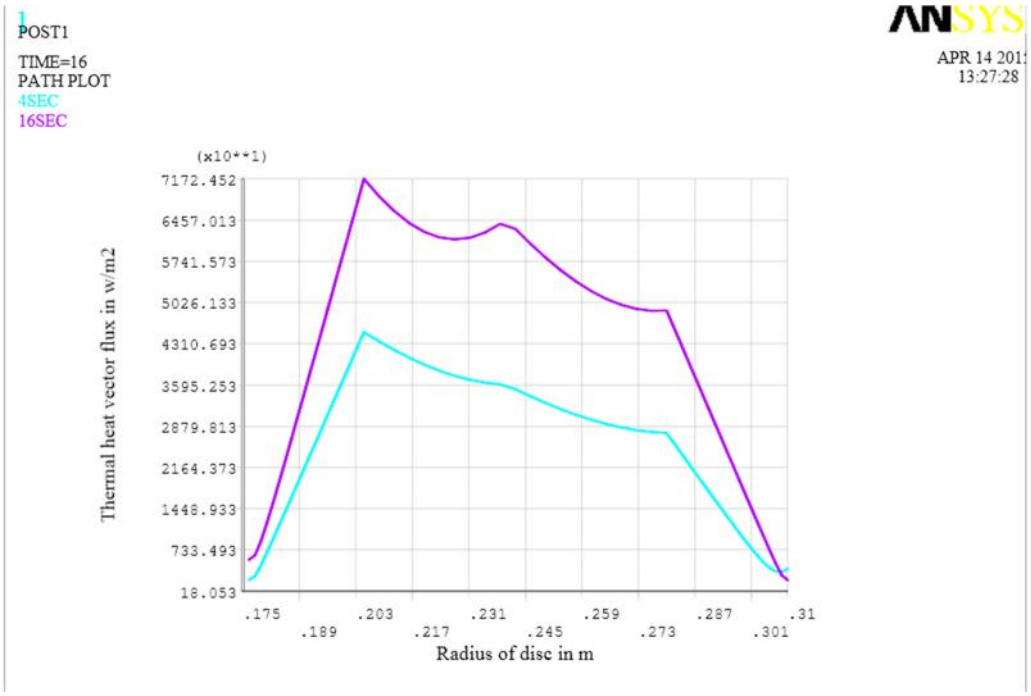

Figure 5.12 Heat Flux Distribution of Orthotropic, 30 mm High Carbon Cast Iron Disc Radius on Friction Surfaces in Two Braking Step

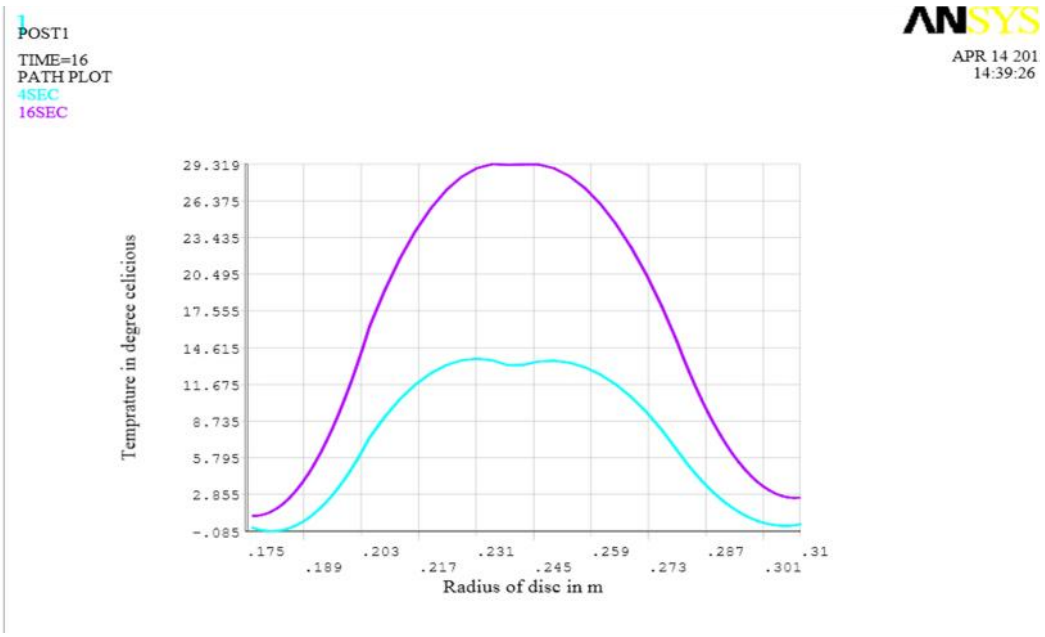

Figure 5.13. Temperature Distribution of Isentropic, 30mm High Carbon Cast Iron Disc Radius on Friction Surfaces in Two Braking Step

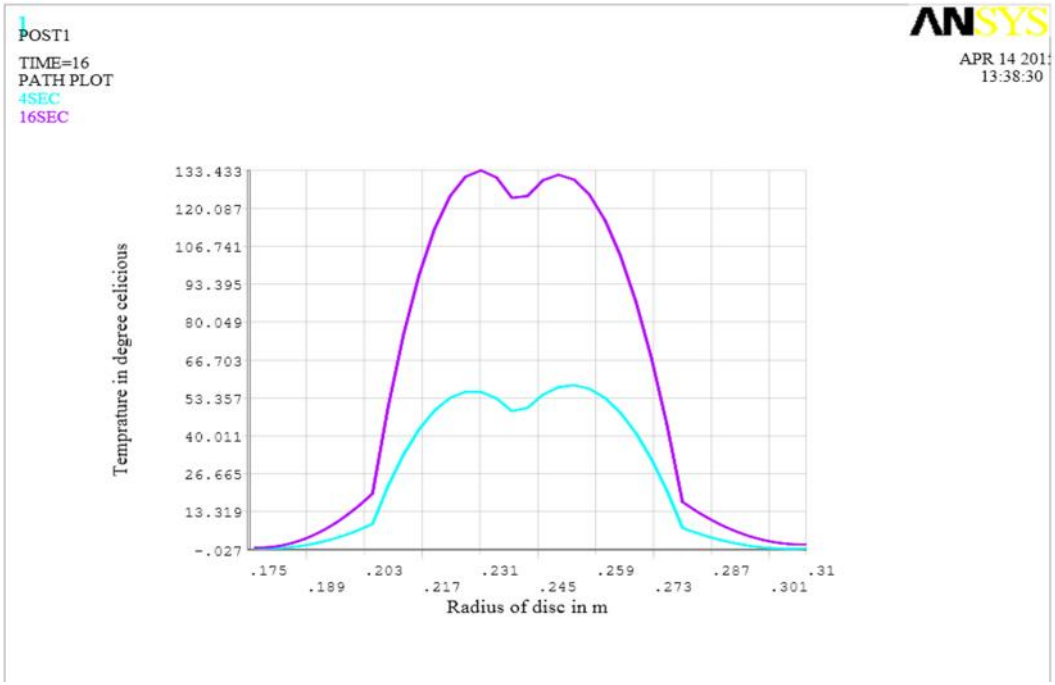

Figure 5.14 Temperature Distributions of Orthotropic, 30 mm High Carbon Cast Iron Disk Radius on Friction Surfaces Two Braking Step

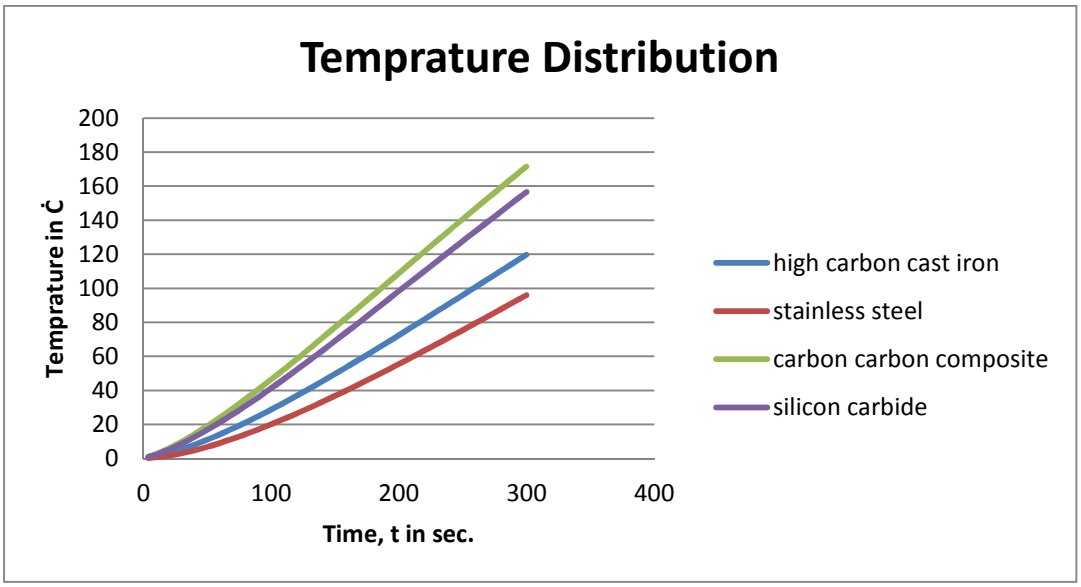

Figure 5.15 Transient Temperature Distributions of the Four Different Materials on Friction Surfaces in Various Operating Braking Time at 300sec.

The above figure 5.15 shows the temperature distribution verses operating braking time on various friction surfaces of four different solid disc brake materials in various braking steps of transient braking .these shows that as time increases the operating temperature increases directly.

As shown in table 6.1, the maximum temperature rise after braking step in stainless steel disc of 30mm flange is 514.268Ċ but the corresponding thermal stress induced at this temperature braking step in high carbon cast iron disc of 30mm flange is 504,448Ċ but the corresponding thermal stresses induced at this temperature are 27.6Mpa(hoop stress), and also we found that the maximum temperature rise in carbon/carbon composite after transient braking step is 513.257Ċ and the thermal stresses induced at this temperature is 28.2Mpa(hoop stresses), silicon carbide has the maximum rise 507.687 and the thermal stresses induced at this temperature has been 67.1Mpa (hoop stress). So we can deduce from thermodynamics consideration in braking in braking system (i.e. the energy dissipated in the form of heat can generate rise in temperature ranging from 300Ċ to 800Ċ).stainless steel materials disc has slightly highest, high carbon cast iron has lowest temperature rise and that we deduce from the above temperature distribution result, all the materials can be considered suitable for braking application hence, considering the possible rise temperature ranging (300Ċ to 800Ċ)

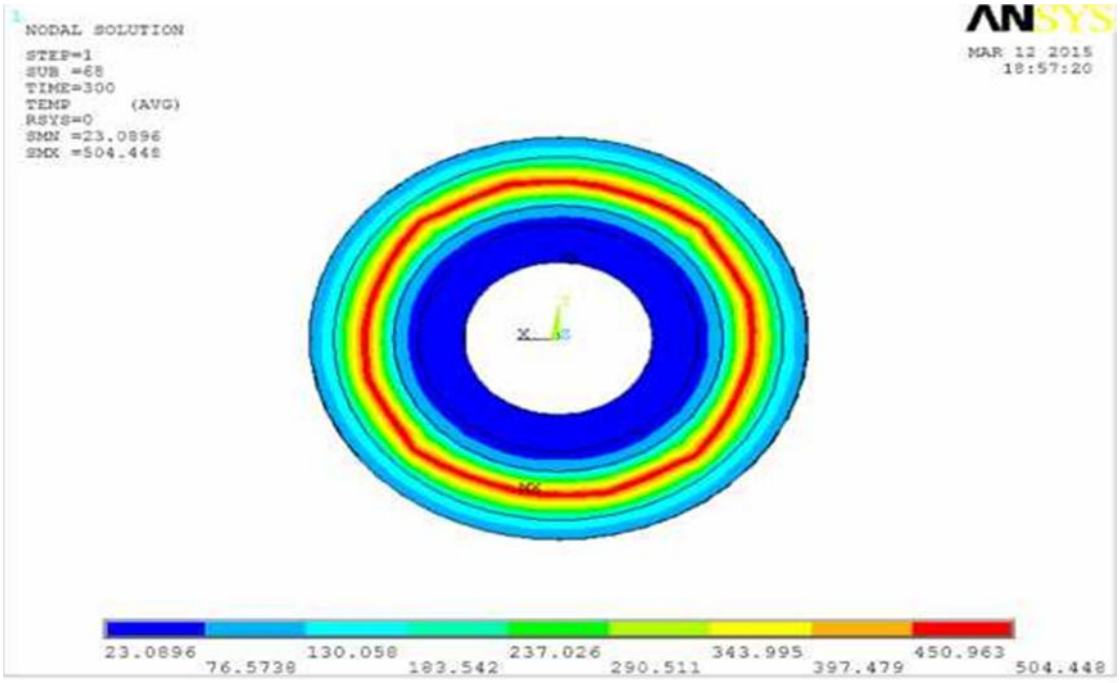

Figure 5.16 Temperature Contours of 30mm High Carbon Cast Iron Disk

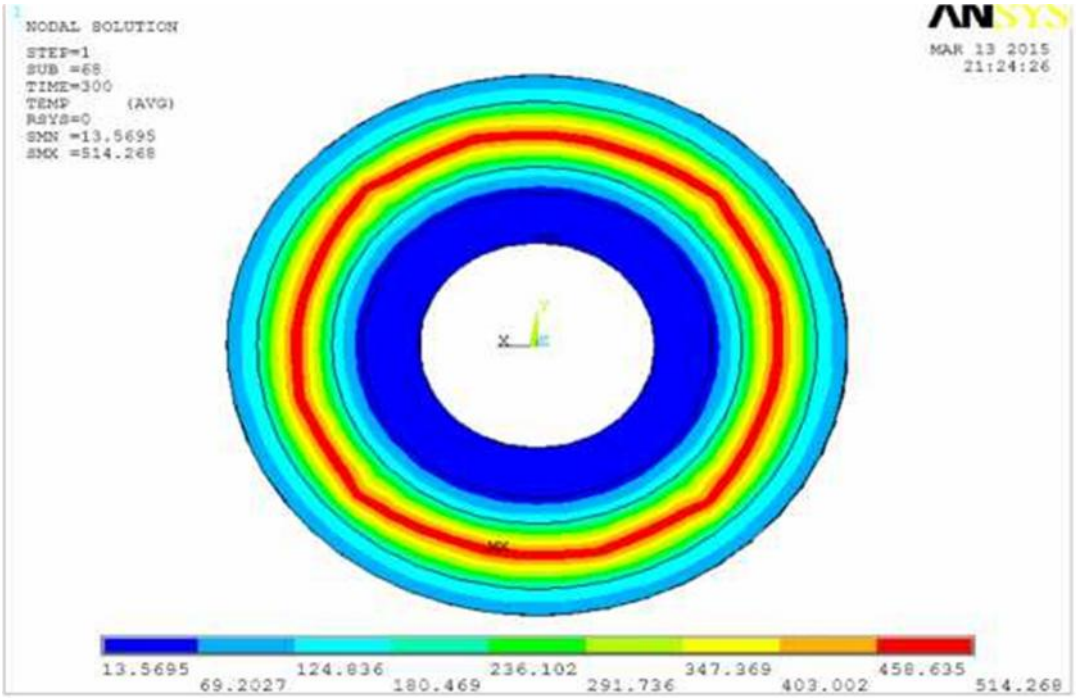

Figure 5.17 Temperature Contours of 30 mm Stainless Steel Disk

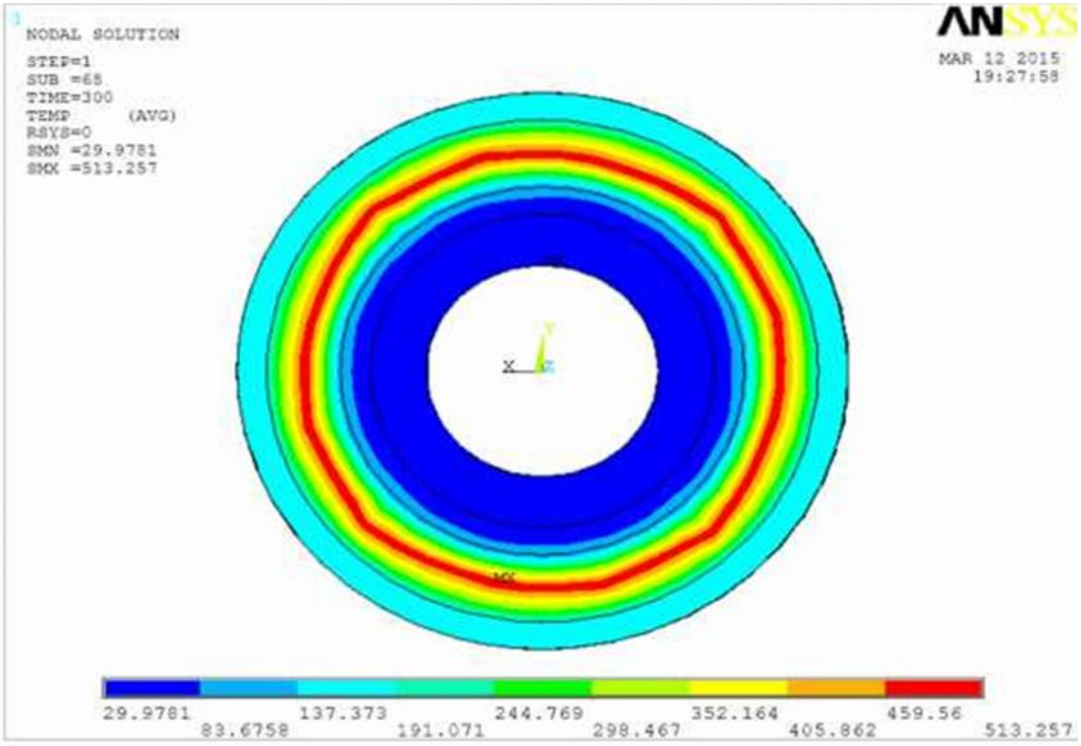

Figure 5.18 Temperature Contours of 30 mm Carbon/Carbon Composite Disk

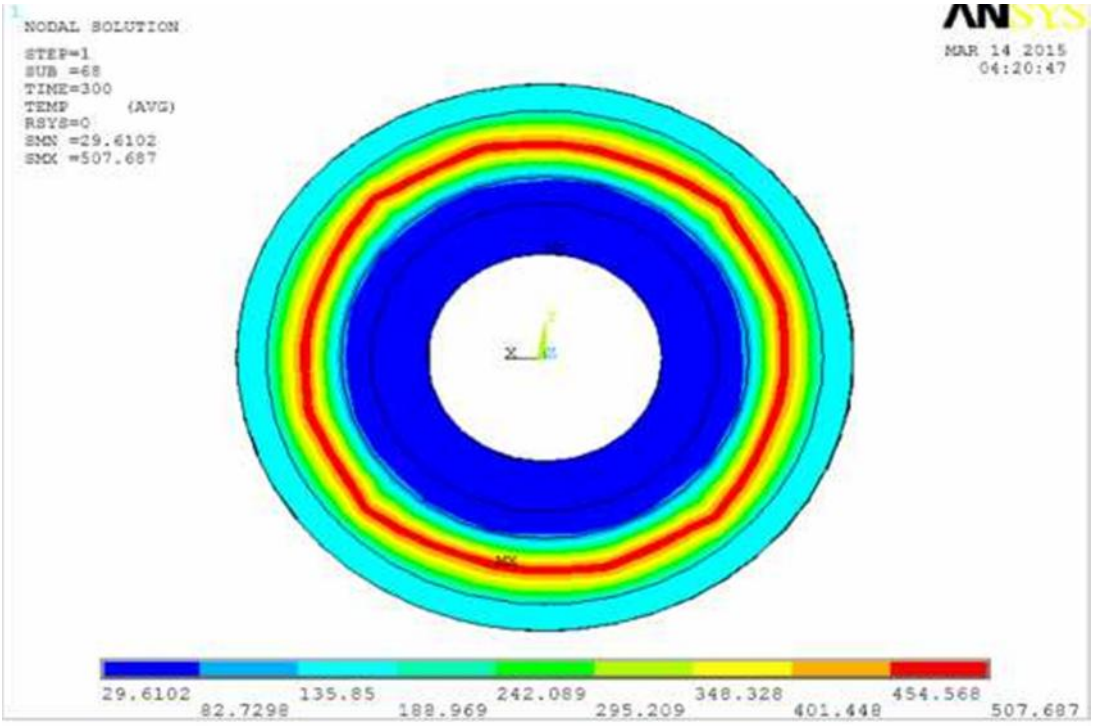

Figure 5.19 Temperature Contours of 30 mm Silicon Carbide Disk

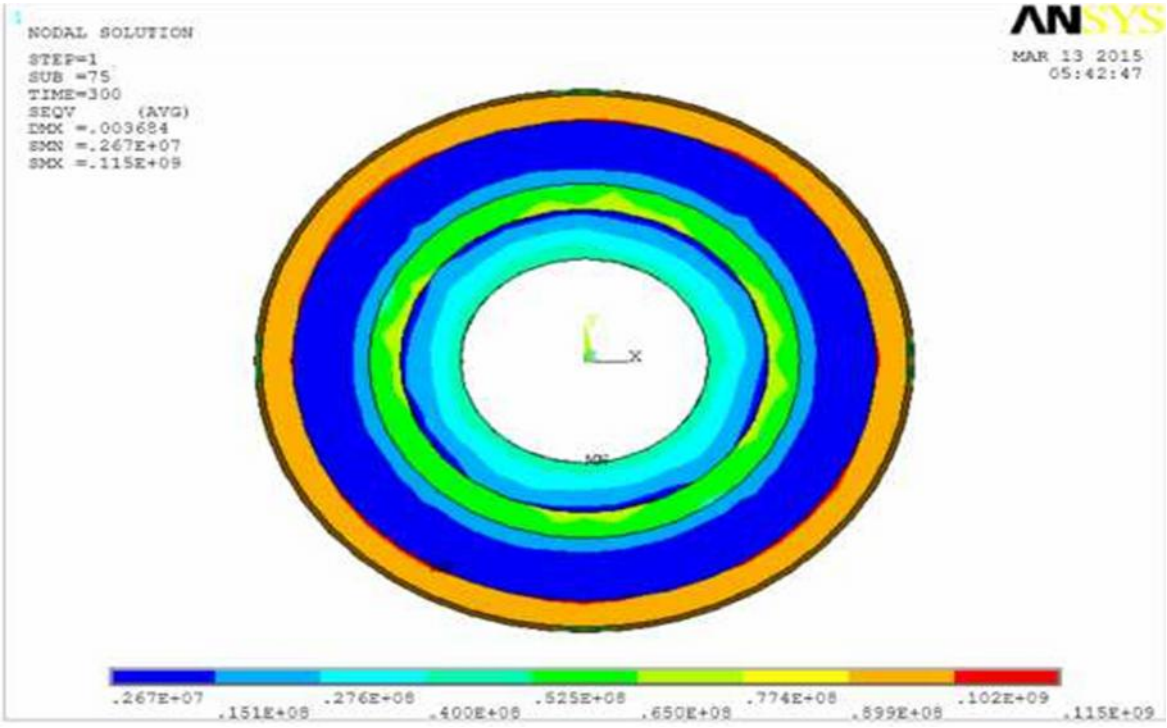

Figure 5.20 Distribution of Von Misses Stress in 30 mm High Carbon Cast Iron Disk

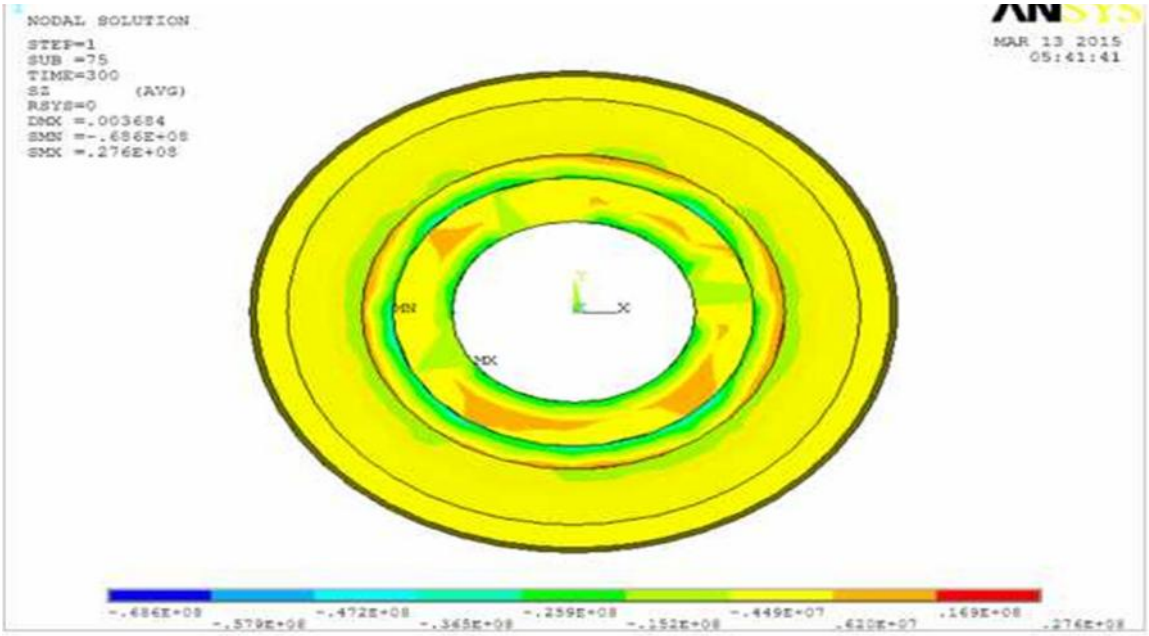

Figure 5.21 Distribution of Hoop Stress in 30 mm High Carbon Cast Iron

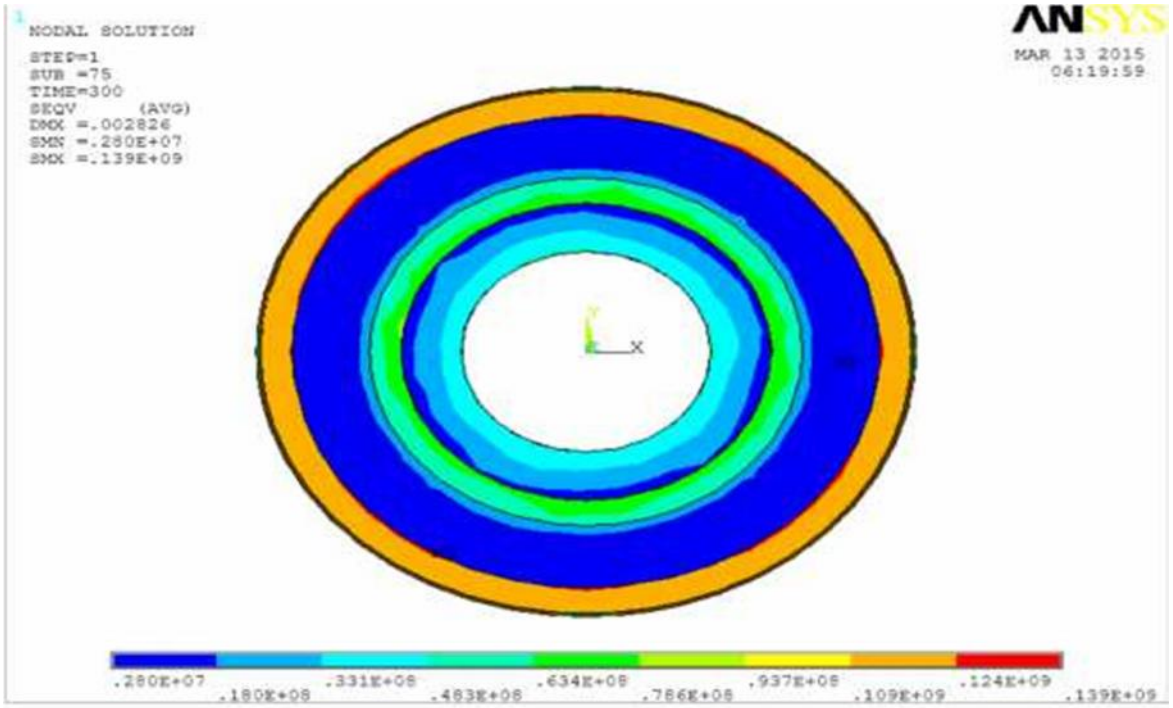

Figure 5.22 Distribution of Von Misses Stress in 30 mm Stainless Steel Disc

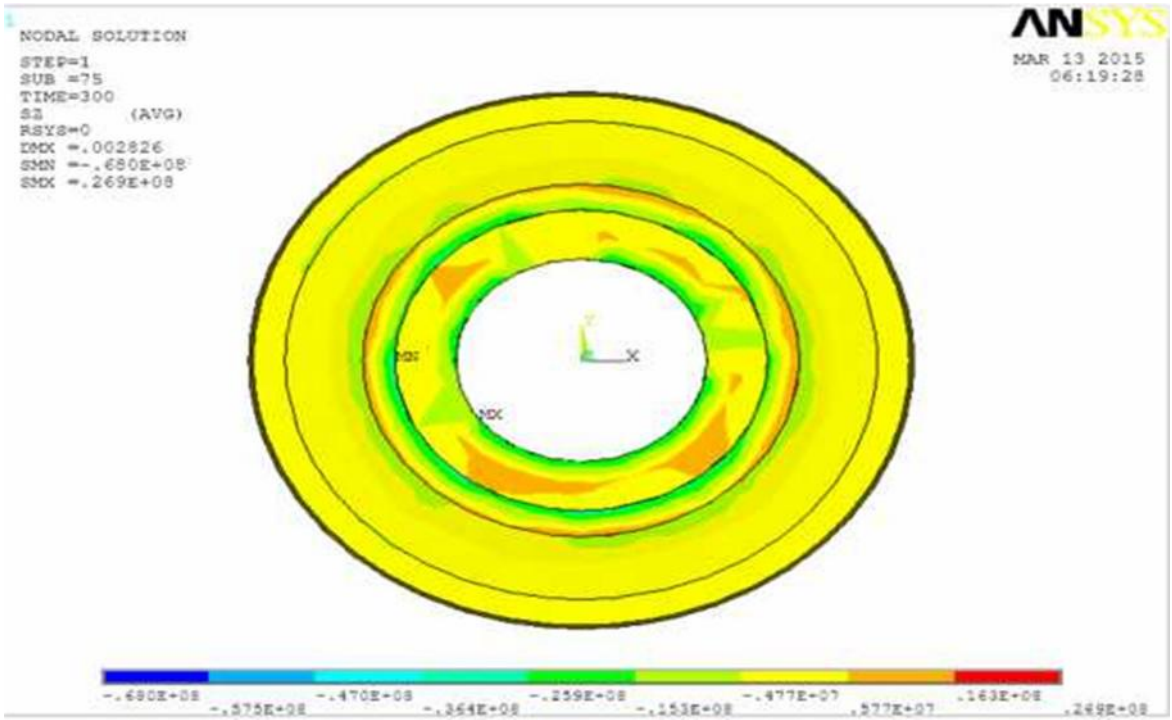

Figure 5.23 Distribution of Hoop Stress in 30 mm Stainless Steel Disk

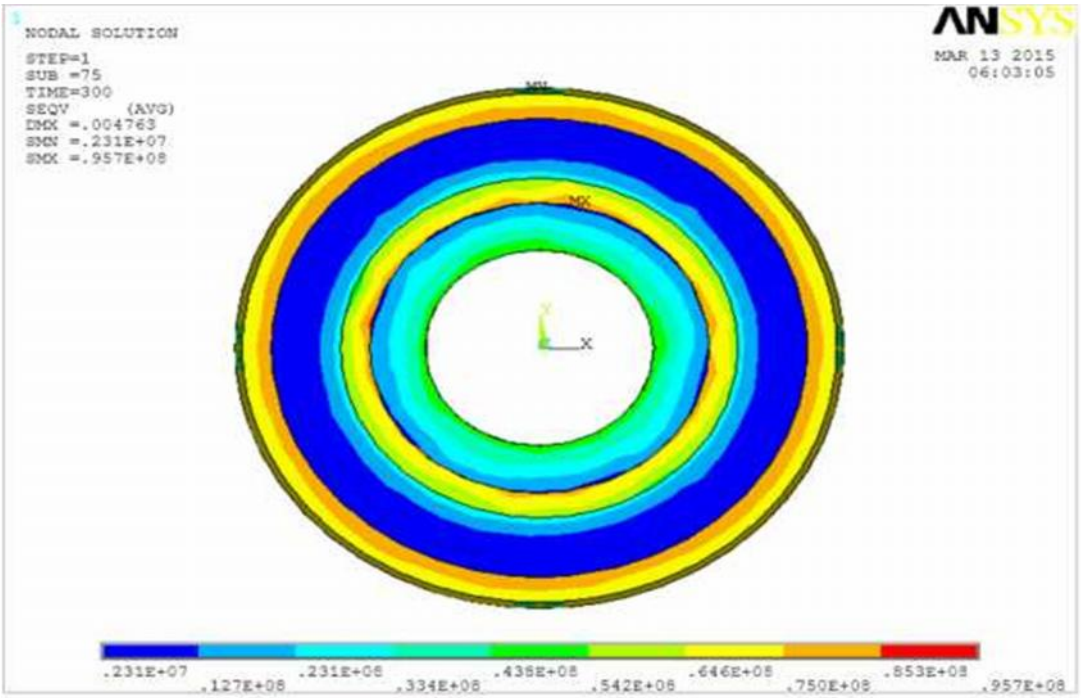

Figure 5.24 Distribution of Von Misses Stress in 30 mm Carbon/Carbon Composite Disk

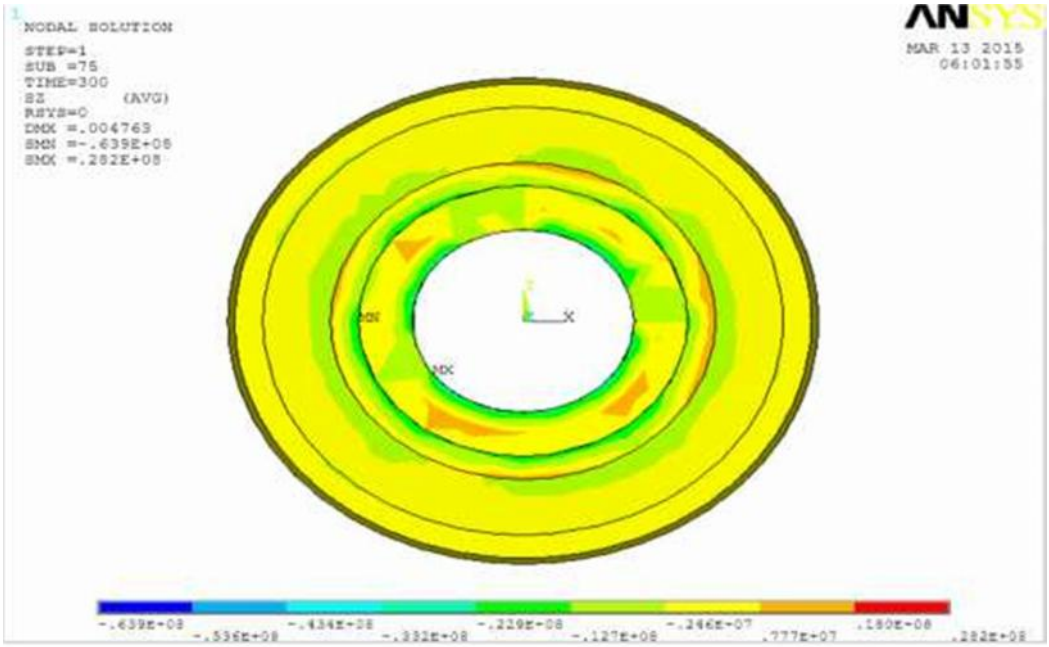

Figure 5.25 Distribution of Hoop Stress in 30 mm Carbon/Carbon Composite Disk

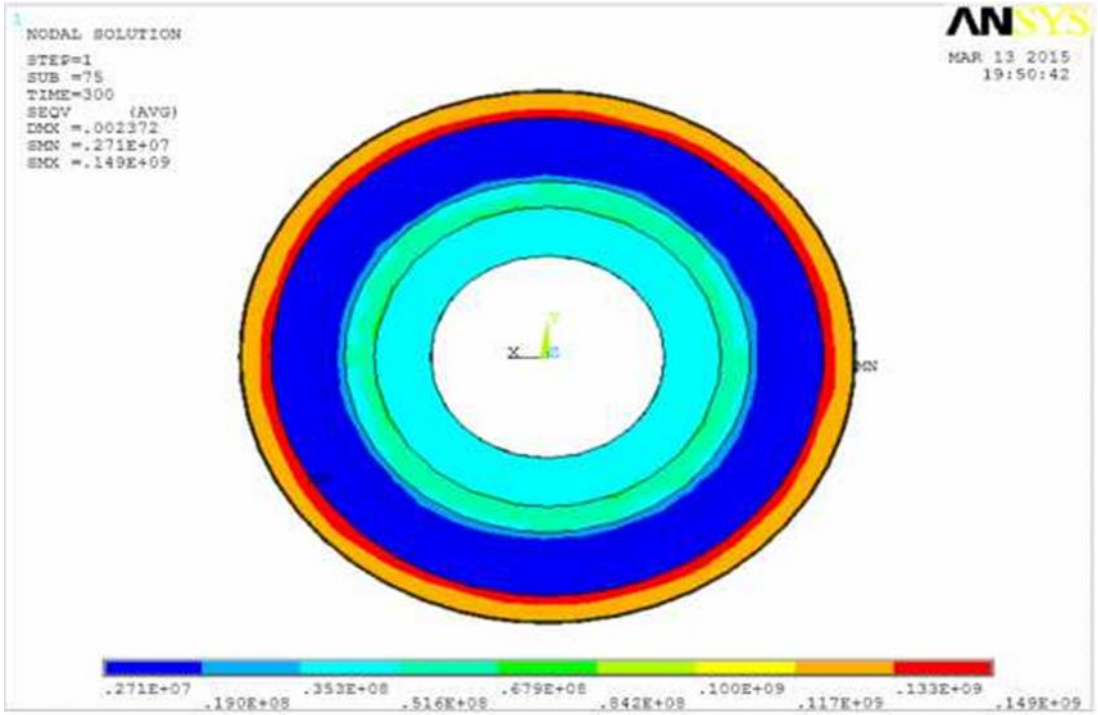

Figure 5.26 Distribution of Von Misses Stress in 30 mm Silicon Carbide Disk

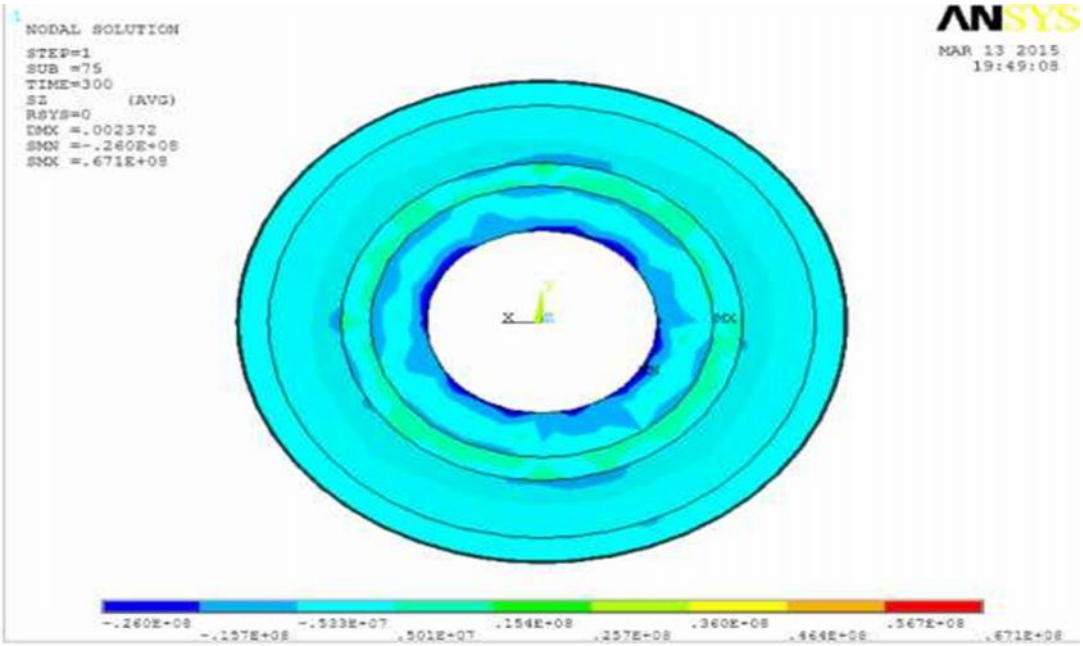

Figure 5.27 Distribution of Hoop Stress in 30 mm Silicon Carbide Disk

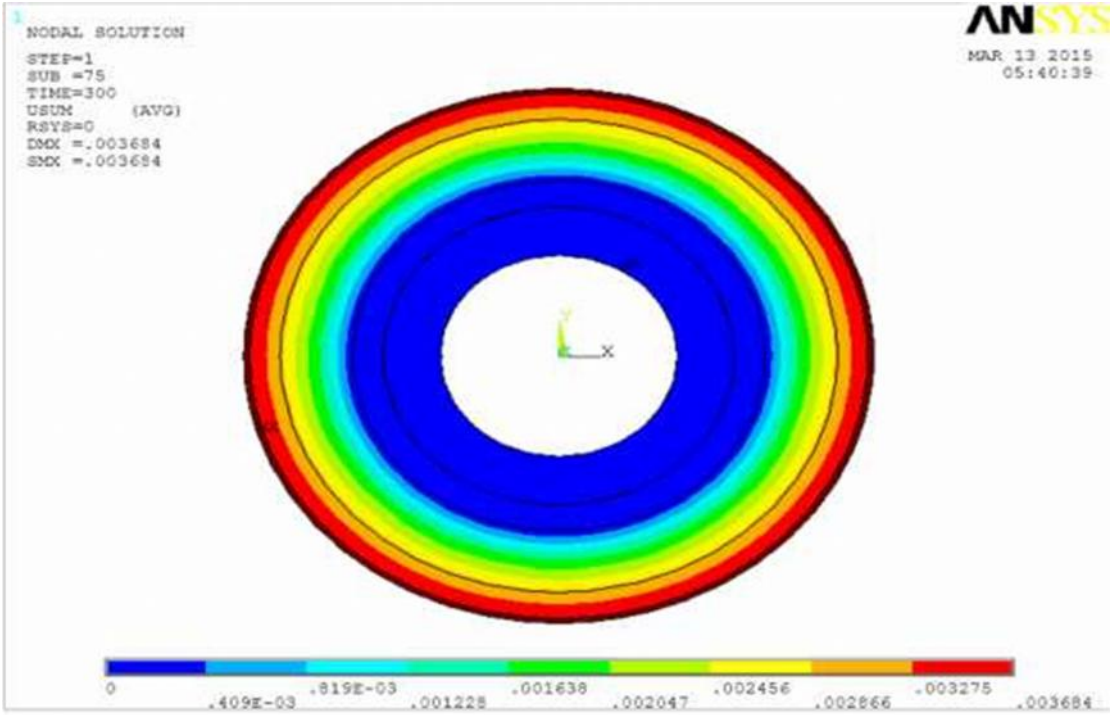

Figure 5.28 Average Displacements in 30mm High Carbon Cast Iron Disk

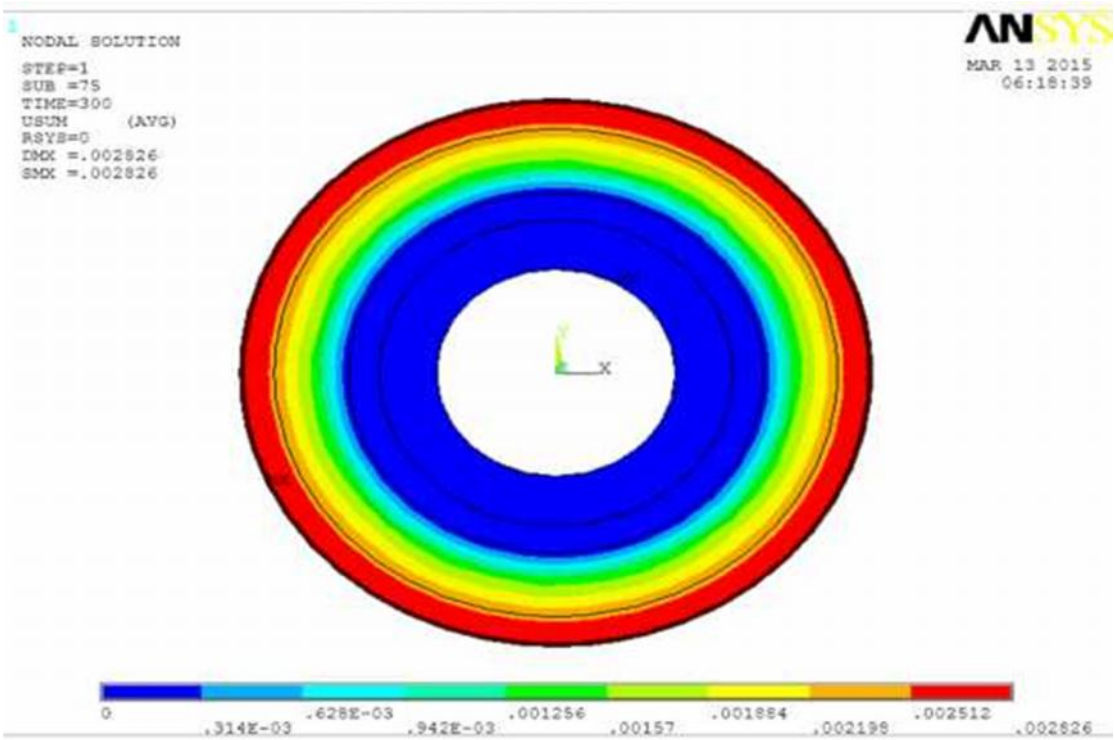

Figure 5.29 Average Displacements in 30 mm Stainless Steel Disk

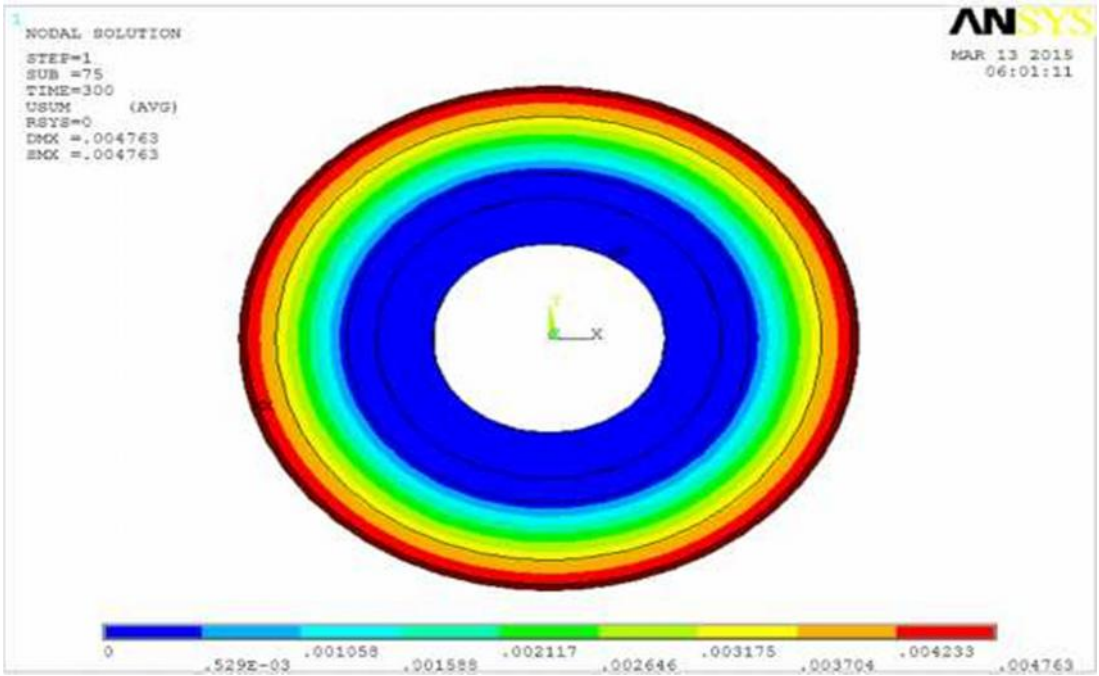

Figure 5.30 Average Displacements in 30mm Carbon/Carbon Composite Disk

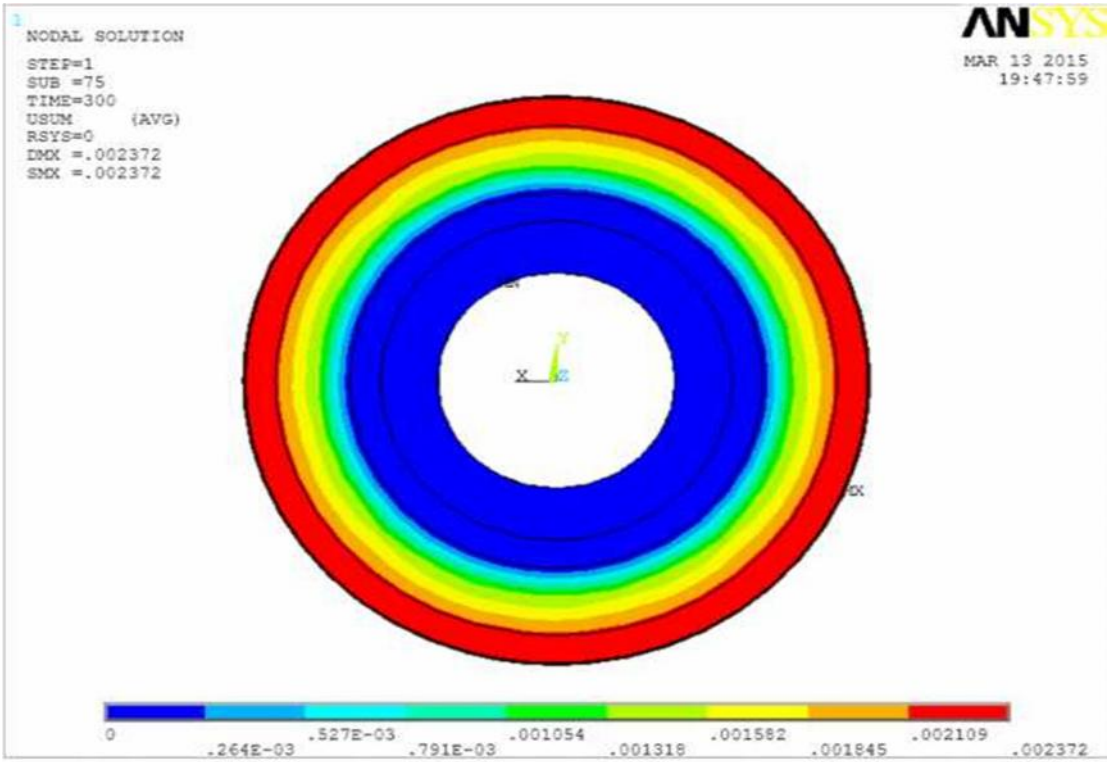

Figure 5.31 Average Displacements in 30mm Silicon Carbide Disk

CHAPTER 6:

CONCLUSIONS and RECOMMENDATIONS

6.1 conclusion

In this paper, the transient thermo elastic analysis of four different disk brake materials in repeated brake applications has been performed. ANSYS software is applied to the thermo elastic contact problem with frictional heat generation. To obtain the simulation of thermo elastic behavior appearing in disk brakes, the coupled heat conduction and elastic equations are solved with contact problems. Also, the fully implicit scheme is used to improve the accuracy of computations in the transient analysis. Through the axis symmetric disk brake model, the TEI phenomenon on each of the friction surfaces between the contacting bodies has been investigated. The hoop stress component in disk brakes has the largest compressive stress value and must be considered as a dominant stress component from the viewpoint of stress failure. The effects of the friction material properties on the contact ratio of friction surfaces are examined and the larger influential properties are found to be the thermal expansion coefficient and the elastic modulus. Based on these numerical results, the thermo elastic behaviors of the four different disk brake materials are also investigated. It is observed that the orthotropic disk brakes can provide better brake performance than the isotropic ones because of uniform and mild pressure distributions.

The present study can provide a useful design tool and improve the brake performance of disk brake system. From Table 6.1 and 6.2 we can say that all the values obtained from the analysis are less than their allowable values. Hence the brake disk design is safe based on the strength and rigidity criteria but out of those stainless steel is the best one.

Comparing the different results obtained from analysis in table 6.1 and 6.2 .It is concluded that disk brake with 30 mm flange width and of material stainless steel is the best possible combination for the present application.

Table 6.1 Conclusions of Material Result

S/N	Brake Disk Materials	Flange Width In (Mm)	Max. Temp Ċ	Min Ċ, Temp	Deflection In Mm	Von Miss Stress		Hoop Stress (Sz)	
						Mpa	Mpa	Mpa	Mpa
1	High Carbon Cast Iron	30	507.69	23	0.00368	115	2.67	67.1	-26
2	Stainless Steel	30	504.45	13.57	0.00283	139	2.8	27.6	-68.6
3	Carbon/Carbon Composite	30	514.27	29.98	0.00476	95.7	2.31	26.9	-68
4	Silicon Carbide	30	513.26	29.61	0.00237	149	2.71	28.2	-63.9

Table 6.2 Allowable Values of Standard Materials

S/N	Brake Material Types	Von Miss Stress	Hoop Stress(Sz)	Yield Stress	Safety Factor
		Mpa Max	Mpa Max	Mpa	n
1	High Carbon Cast Iron	115	27.6	130	1.1304347
2	Stainless Steel	139	26.9	520	3.741007194
3	Carbon/Carbon Composite	95.7	28.2	150	1.567398119
4	Silicon Carbide	149	67.1	300	2.013422819

- from table 6.2 even if all analyses are less than their allowable values we conclude that stainless steel is safer than others.

6.2 RECOMMENDATIONS

From the analyses conclusion, to fill further research the gaps I recommend the following.

- To get best and accurate result the effect of thermal and structural combined result has to be shown together
- The analysis has to be investigated by considering variable thermal conductivity and variable specific heat to be generalized the overall results
- Also I recommend the disc materials to be heterogeneous and see the effects including the ventilated case this and above mentioned will make the thesis more complete and will be future investigations.

REFERENCE

1. Brilla, J. Laplace Transform and New Mathematical Theory of Visco Elasticity, Vol. 32, (1997).

2. Lin, J. -Y. And Chen, H. -T. Radial Axis Symmetric Transient Heat Conduction in Composite Hollow Cylinders with Variable Thermal Conductivity, Vol. 10, (1992).

3. Kennedy, F. E., Colin, F. Floquet, A. And Glovsky, R. Improved Techniques For Finite Element Analysis of Sliding Surface Temperatures. Westbury House (1984).

4. Tsinopoulos, S. V, Agnantiaris, J. P. And Polyzos, D. An Advanced Boundary Element/Fast Fourier Transform Axis Symmetric Formulation for Acoustic Radiation and Wave Scattering Problems, J.Acoust. Soc. Amer., Vol105, (1999).

5. Gonska, H. W. And Kolbinger, H.J.Temperature and Deformation Calculation of Passenger Car Brake Disks, Proc. Abaqus User's Conference Aachen, Germany, (1993).

6. Floquet, A. And Dubourg, M.-C. Non Axis Symmetric Effects for Three Dimensional Analyses of a Brake, Asme J. Tribology, Vol. 116, (1994).

7. Burton, R. A. Thermal Deformation In Frictionally Heated Contact, Wear, Vol. 59, (1980).

8. Anderson, A. E. And Knapp, R. A. Hot Spotting In Automotive Friction System Wear, Vol.135, (1990).

9. Comninou, M. And Dundurs, J. On The Barber Boundary Conditions for Thermo Elastic Contact, ASME J, Vol. 46, (1979).

10. Barber, J. R. Contact Problems Involving a Cooled Punch, J. Elasticity, Vol. 8,

11. Barber, J. R. Stability of Thermo Elastic Contact, Proc. International Conference on Tribology, P Institute of Mechanical Engineers, (1987).

12. Dow, T. A. And Burton, R. A. Thermo Elastic Instability of Sliding Contact In The Absence of Wear, Wear, Vol. 19, (1972).

13. Lee, K. And Barber, J.R. Frictionally-Excited Thermo Elastic Instability In Automotive Disk Brakes, ASME J. Tribology, Vol. 115, (1993).

14. Lee, K. And Barber, J. R. An Experimental Investigation Of Frictionally- Excited Thermo Elastic Instability In Automotive Disk Brakes Under A Drag Brake Application, Asme J. Tribology, Vol. 116, (1994).

15. Lee, K. And Barber, J. R. Effect of Intermittent Contact on the Stability of Thermo Elastic Contact, Asme J. Tribology, Vol. 198, (1995).

16. Zagrodzke, S, Barber, J. R. And Hulbert, G.M. Finite Element Analysis Of Frictionally Excited Thermo Elastic Instability, J. Thermal Stresses, Vol. 20, (1997).

17. Leroy, J. M. Floquet, A. And Villechaise, B. Thermo-Mechanical Behavior of Multilayered Media: Theory, Asme J. Tribology, and Vol. 111, (1989).

18. Beeker, A.A. The Boundary Element Method in Engineering, Mcgraw-Hill, New York, (1992).

19. Akin, J. E. Application and Implementation of Finite Element Methods, Academic Press, Orlando, Fl, (1982).

20. Zagrodzki, P. Analysis of Thermo Mechanical Phenomena in Multi Disk Clutches And Brakes, Wear 140, (1990).

21. Cook, R. D. Concept and Applications of Finite Element Analysis, Wiley, Canada, (1981).

22 Zienkiewicz, O. C. The Finite Element Method, Mcgraw-Hill, New York, (1977).

23. Wang, H. -C. And Banerjee, P. K. Generalized Axis Symmetric Elastodynamic Analysis By Boundary Element Method, Vol. 30, (1990).

24. V.M.M.Thilak, Transient Analysis of Rotor Disc of Disc Brake Using Ansys, Mechanical Engineering, S.N.S.College of Engineering- Coimbatore-641107

25. G. Babukanth & M. Vimal Teja, Transient Analysis Of Disk Brake By Using Ansys Software, Nimra College Of Engineering & Technology, Ibrahim patnam, Vijayawada.Issn No2231-6477 Volume1,Issue 2012.

26. Oder, G.; Reibenschuh, M.; Lerher, T.; Šraml, M.; Šamec, B.; Potrč, I. Thermal and Stress Analysis of Brake Discs In Railway Vehicles, Advanced Engineering 3(2009)1, Issn 1846-5900.

27. Akara Sawardsuk, Saiprasit Koetniyom, Design and Development of Thai Railway Brake Disc under Temperature Analysis, International Journal of Engineering Science and Innovative Technology, Volume 2, Issue 1, January 2013

28. V.M.M.Thilak, R.Krishnaraj, Dr.M.Sakthivel, K.Kanthavel, Deepan Marudachalam M.G, R.Palani Transient Thermal and Structural Analysis of the rotor Disk of rotor Disk. International Journal of Scientific and Engineering Research Volume2, Issue8, August 2011, Issn2229-5518